Stress Corrosion Cracking of Low-Alloy RPV Steels under BWR Conditions - New Observations -

H.P. Seifert, S. Ritter

Paul Scherrer Institut

Nuclear Energy and Safety Research Department

Laboratory for Materials Behaviour

CH-5232 Villigen PSI

Tel.: ++41 56 310 44 02   Fax: ++41 56 310 21 99   E-mail: hans-peter.seifert@psi.ch

Presented at ICG-EAC Meeting, April 23 – 27, 2001, Kyongju, Korea

Outline

- SCC II programme (1996 – 1999)
  - Summary and conclusions
  - Open questions
- Materials and experimental set-up
- Results and discussion
  - Effect of temperature
  - Ripple loading
- Conclusions

EAC of RPV Steels

	EAC		
Mechanism	**SCC** **S**tress **C**orrosion **C**racking	**SICC** **S**train-**I**nduced **C**orrosion **C**racking	**CF** **C**orrosion **F**atigue
Type of loading	static	slow monotonically rising or very low-cycle (vLCF)	cyclic low-cylce high-cycle
Data	K_{ISCC}, da/dt	da/dt, N_i, da/dN	N_i, da/dN, $K_{I,th}$
LWR operation condition	steady-state power operation	start-up/shut-down thermal stratification	thermal fatigue thermal stratification vibrations
Quantitative characterisation	BWR VIP disposition lines	-	ASME III and XI
Programmes	SpRK II CASTOC	RIKORR CASTOC	CASTOC

Summary and Conclusions from SCC II

- **No susceptibility** to SCC crack growth under **purely static loading** conditions:

  - for small scale yielding conditions

    and

  - if water chemistry conditions ≡ current BWR/NWC operation practice (EPRI water chemistry guidelines)

- **Fast** and **sustained SCC crack growth** cannot be excluded:

  - for **faulted water chemistry conditions** (> EPRI Action Level 3)

    and/or

  - if a **positive strain rate** at crack front can be maintained under external static loading by either **gross ligament yielding** of specimens with **high net section stress** or loading of specimens **near to** $\mathbf{K_{IJ}}$.

Restrictions:

• T ≈ 288 °C • RPV base metal, Q + T + SR • pure static loading

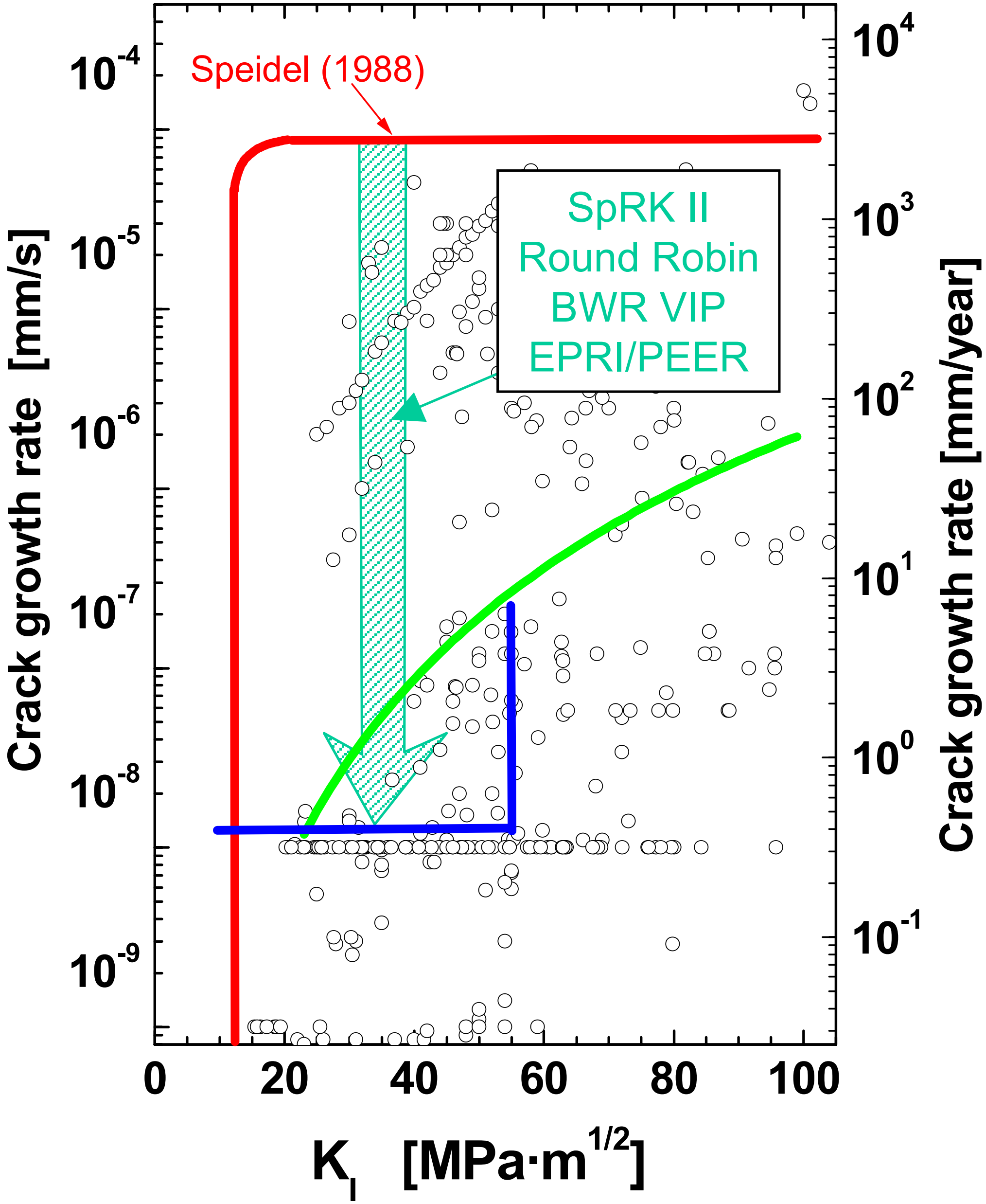

J. Heldt, H.P. Seifert, Nucl. Eng. & Design, Vol. 206 (2001), pp. 57 – 89.

H.P. Seifert, J. Heldt et al., BFE Final Report, February 2000.

D. Blind et al., „European Round Robin Test on EAC of LAS under BWR Conditions“, 9th Int. Symp. on Env. Degr. of Mat. in Nuclear Power Systems - Water Reactors, pp. 911 – 919, ANS/NACE/TMS, Newport Beach, CA, USA, 1999.

F.P. Ford et al., “Stress corrosion cracking of low alloy steels under BWR conditions; assessment of crack growth rate algorithms“, 9th Int. Symp. on Env. Degr. of Mat. in Nucl. Power Systems – Water Reactors, pp. 855 – 863, Newport Beach, CA, USA, TMS, ANS, NACE, 1999.

K. Kussmaul et al., Nucl. Eng. & Design, Vol. 168 (1997), pp. 53 - 75.

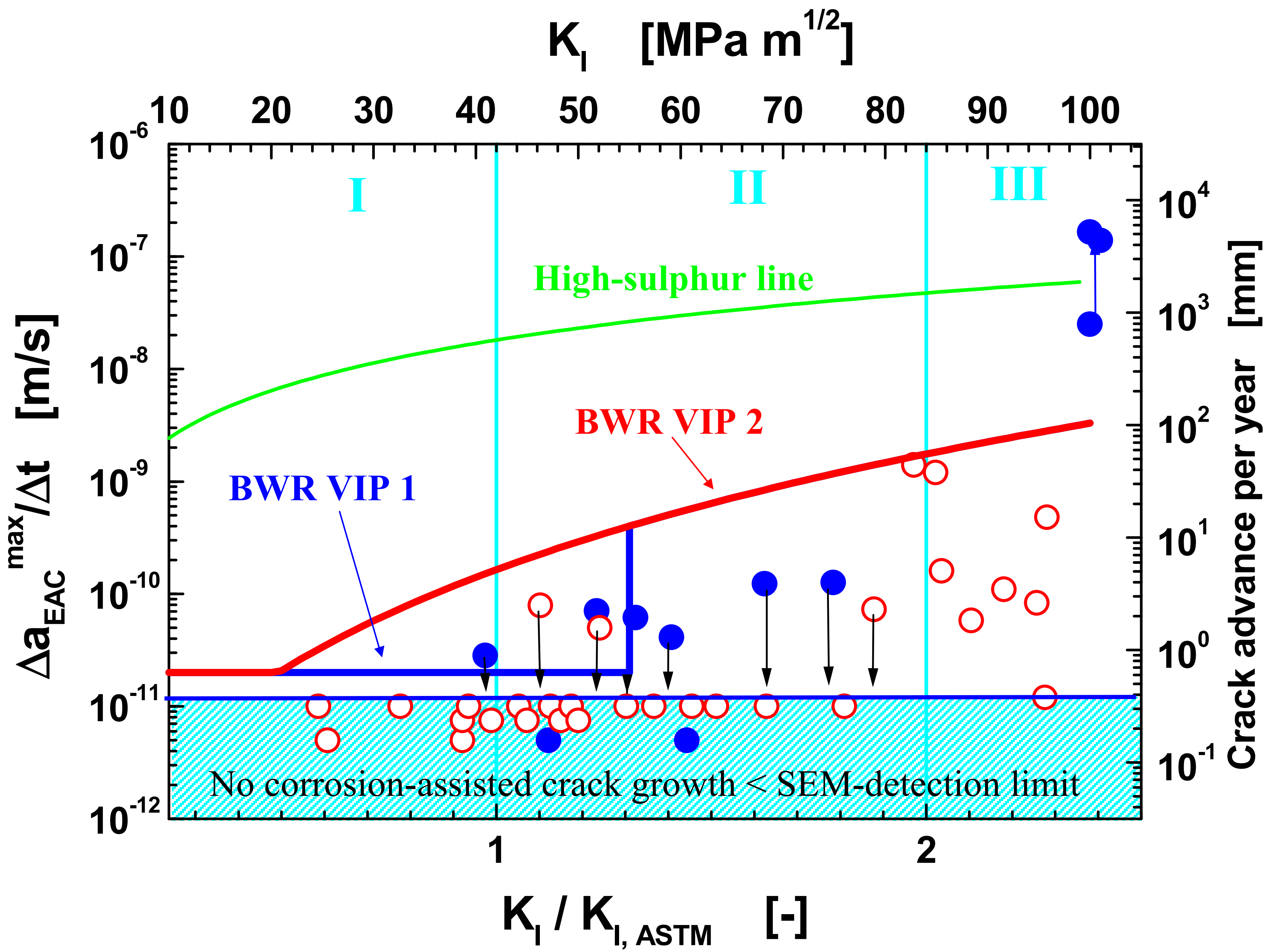

K_I [MPa m$^{1/2}$]
10 20 30 40 50 60 70 80 90 100
I
II
III
High-sulphur line
BWR VIP 2
BWR VIP 1
No corrosion-assisted crack growth < SEM-detection limit
$\Delta a_{EAC}^{max}/\Delta t$ [m/s]
10^{-6} 10^{-7} 10^{-8} 10^{-9} 10^{-10} 10^{-11} 10^{-12}
Crack advance per year [mm]
10^{4} 10^{3} 10^{2} 10^{1} 10^{0} 10^{-1}
1 2
$K_I / K_{I, ASTM}$ [-]

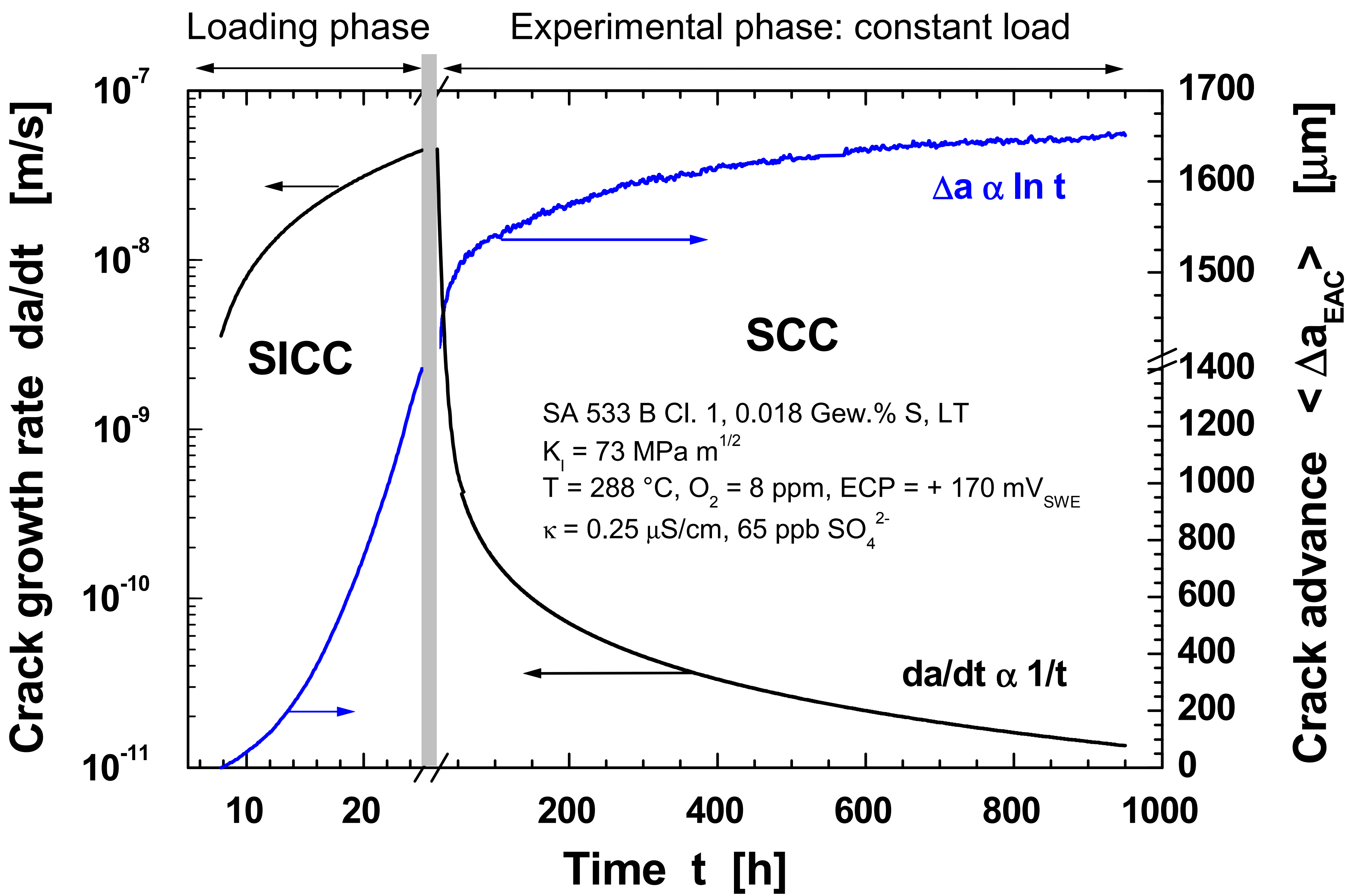
Loading phase
Experimental phase: constant load
SICC
SCC
Δa α ln t
da/dt α 1/t
SA 533 B Cl. 1, 0.018 Gew.% S, LT
K_I = 73 MPa m^1/2
T = 288 °C, O_2 = 8 ppm, ECP = + 170 mV_SWE
κ = 0.25 µS/cm, 65 ppb SO_4^2-
Crack growth rate da/dt [m/s]
10^-7
10^-8
10^-9
10^-10
10^-11
Crack advance < Δa_EAC > [µm]
1700
1600
1500
1400
1200
1000
800
600
400
200
0
10
20
200
400
600
800
1000
Time t [h]

Open Questions

- Long-term SCC cracking behaviour under constant active load
  no long-term tests ≥ 1 a under oxidising BWR conditions
- Effect of temperature
- SCC susceptibility of RPV weld material
- SCC susceptibility of coarse grain zone of RPV weld HAZ
  very limited number of tests with weld HAZ, location of pre-crack
- Ripple loading (R ≥ 0.95)
  thermal and pressure fluctuations during stationary power operation
- Effect of short-term water chemistry transients
  effect of short-term SO_4^{2-}, Cl^- -transients under oxidising conditions on long-term cracking behaviour (response times, memory effects, ...)

Investigated Materials

Material	Regulation Standard	S [wt.%]	Al [wt.%]	Similar to
20 MnMoNi 5 5	KTA 3201.1	0.004	0.013	SA 508 Cl. 3
22 NiMoCr 3 7	KTA 3201.1	0.007	0.018	SA 508 Cl. 2
SA 508 Cl. 2	ASME BPV Code Section II, Part A	0.004	0.015	22 NiMoCr 3 7
SA 533 B Cl. 1	ASME BPV Code Section II, Part A	0.018	0.03	20 MnMoNi 5 5
RPV weld		0.007	0.0053	

Steel		C	Si	Mn	P	S	Cr	Mo	Ni	V	Al	Cu
20 MnMoNi 5 5	A	0.15	0.29	1.40	0.005	0.005	0.14	0.51	0.65	0.007	0.036	-
20 MnMoNi 5 5	B	0.21	0.25	1.26	0.004	0.004	0.15	0.5	0.77	0.008	0.013	0.06
20 MnMoNi 5 5	C	0.19	0.2	1.39	0.008	0.010	0.14	0.53	0.53	0.009	0.04	0.08
SA 533 B Cl. 1	D	0.25	0.24	1.42	0.006	0.018	0.12	0.54	0.62	0.007	0.03	0.15
20 MnMoNi 5 5	E	0.20	0.16	1.24	0.008	0.009	0.09	0.50	0.78	0.010	0.01	0.06
SA 508 Cl. 2	F	0.21	0.27	0.69	0.005	0.004	0.38	0.63	0.78	0.006	0.015	0.16

		Room temperature				288 °C	
Steel		$R_{P0.2}$ [MPa]	R_m [MPa]	A_5 [%]	Z [%]	$R_{P0.2}$ [MPa]	Heat treatment
20 MnMoNi 5 5	A	553	669	22.3	74.5	-	as received
20 MnMoNi 5 5	B	485	648	19.3	72.1	418	910 °C - 920 °C / 6 h / WQ / 640 °C - 650 °C / 9.5 h / FC
20 MnMoNi 5 5	C	565	684	19.6	73.5	-	910 °C - 920 °C / 6 h / WQ / 640 ° C - 650 °C / 9.5 h / Air
SA 533 B Cl. 1	D	468	616	21.0	43.0	411	915 °C / 12 h / 860 °C / 12 h / WQ / 635 °C / 12 h / FC
20 MnMoNi 5 5	E	475	619	22.7	63.6	444	910 °C - 920 °C / 4.5 h/ WQ / 640 °C - 645 °C / 9 h/ FC
SA 508 Cl. 2	F	448	611	17.9	71.0	396	as received

High-Temperature Water Loop

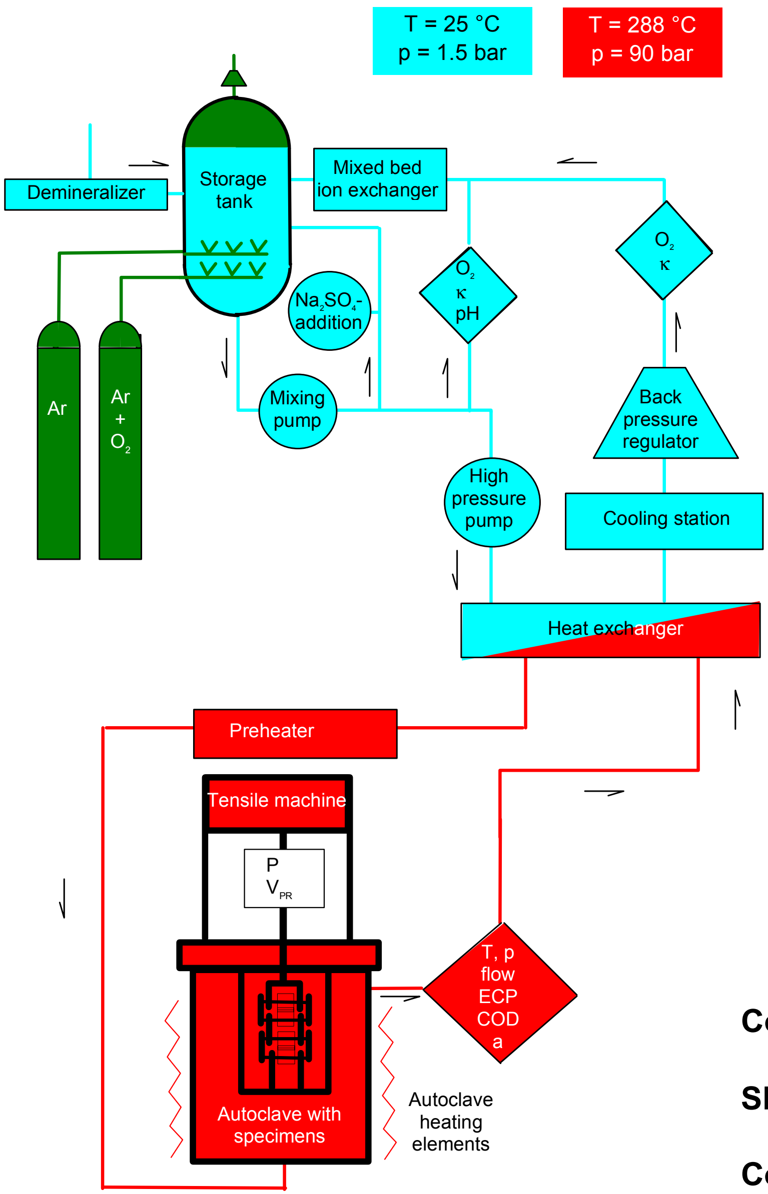

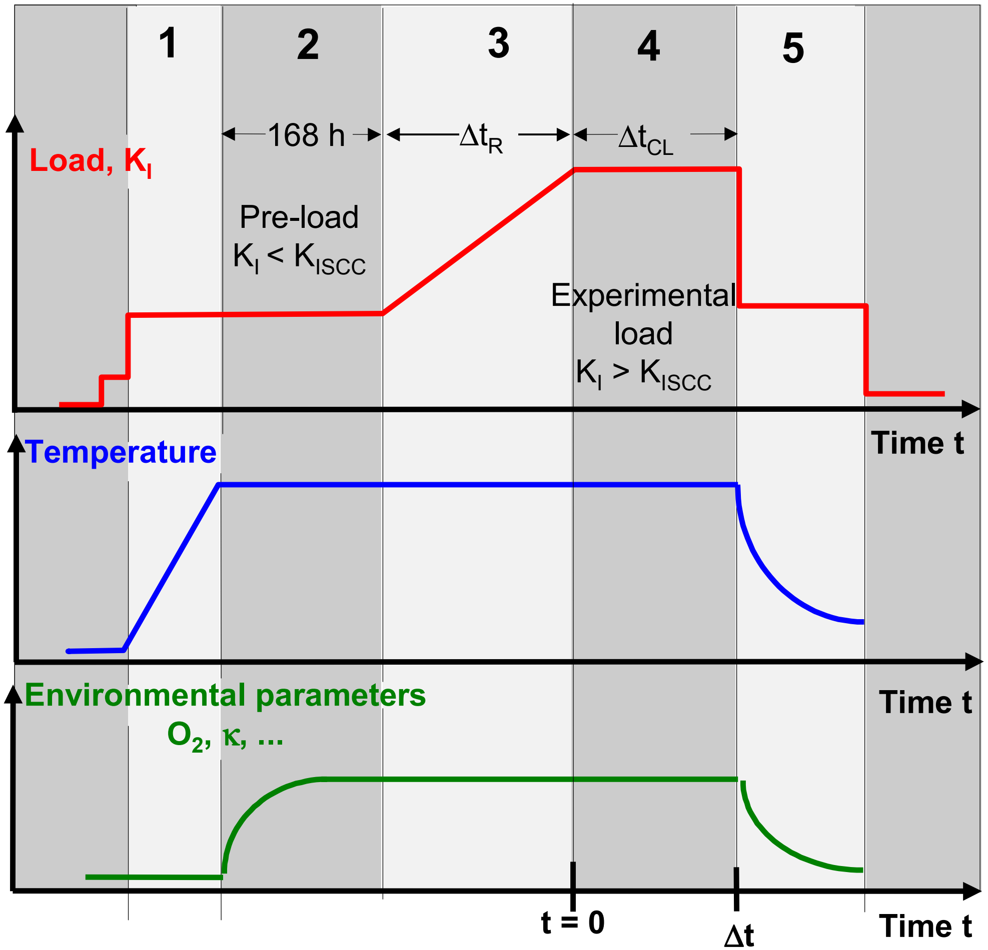

1:Heating phase 2: Conditioning phase

3: Slow rising load phase (Δt_R) 4: Constant load phase

Conditioning phase: - formation of an uniform oxide film

- stable and constant environmental parameters

SRL phase 3 : Generation of an actively growing EAC crack: $da/dt > da/dt_{crit}$, $\Delta a > \Delta a_{crit}$

$da_{SICC}/dt = da_{SCC}/dt\ (t = 0) = 1E\text{-}10$ to $1E\text{-}7$ m/s

Constant load phase 4: Start of CL-phase with actively growing EAC crack

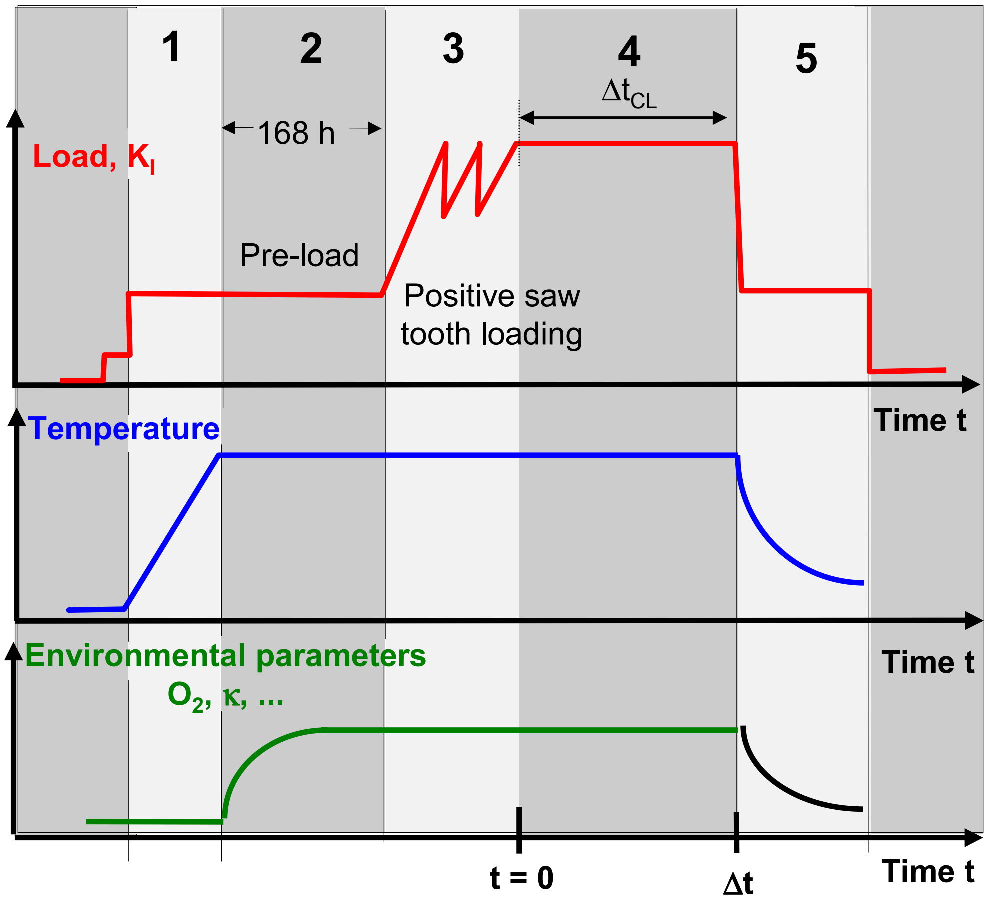

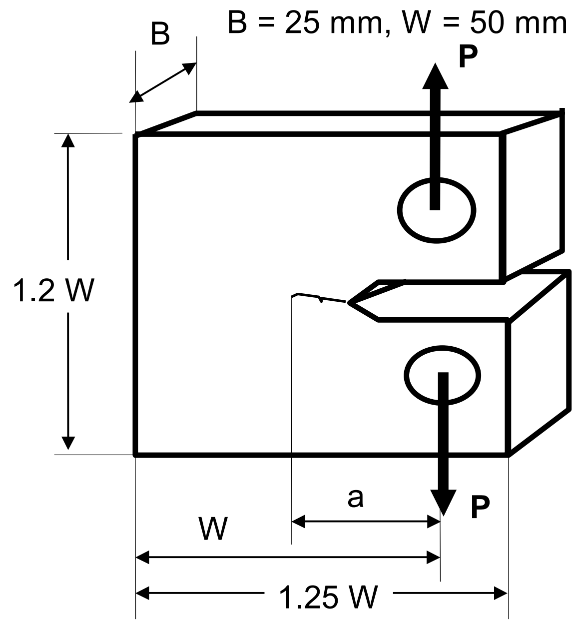

$$K_I = \frac{P}{B \cdot \sqrt{W}} \cdot f\left(\frac{a}{W}\right)$$

1:Heating phase 2: Conditioning phase 3: Low-cycle fatigue phase
4: Constant load phase (Δt_{CL}) 5: Cooling phase

$$f\left(\frac{a}{W}\right) = \frac{\left[2 + \frac{a}{W}\right] \cdot \left[0.886 + 4.64 \cdot \left(\frac{a}{W}\right) - 13.32 \cdot \left(\frac{a}{W}\right)^2 + 14.72\left(\frac{a}{W}\right)^3 - 5.6 \cdot \left(\frac{a}{W}\right)^4\right]}{\left[1 - \frac{a}{W}\right]^{1.5}}$$

Conditioning phase: - formation of an uniform oxide film
- stable and constant environmental parameters

LCF phase 3: Generation of an actively growing EAC crack: $da/dt > da/dt_{crit}$, $\Delta a > \Delta a_{crit}$
$da_{LCF}/dt = da_{SCC}/dt\ (t = 0) = 3E-10$ to $1E-8$ m/s

Constant load phase 4: Start of CL-phase with actively growing EAC crack

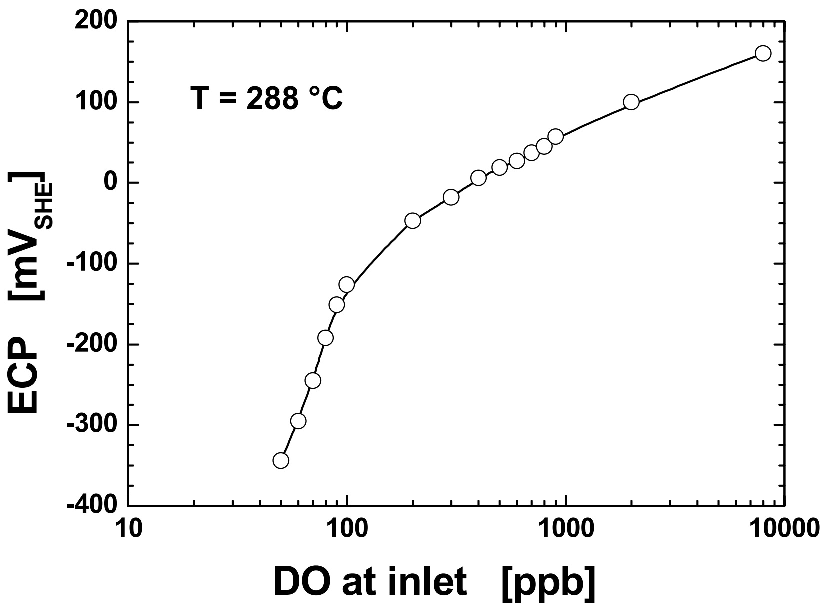

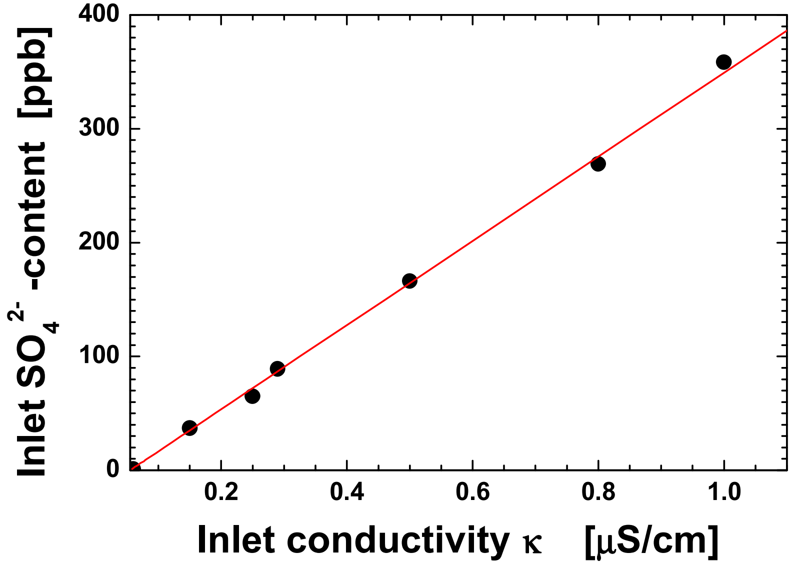

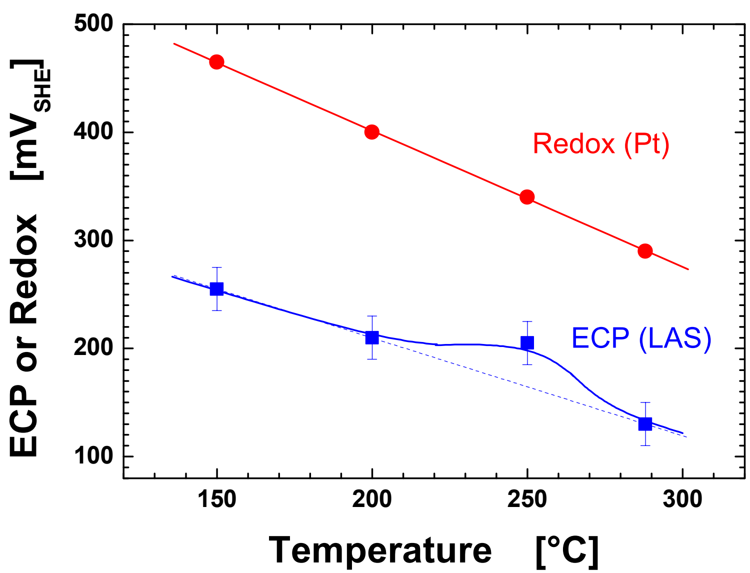

Ion chromatography [ppb]

	SO_4^{2-}	Cl^-	NO_3^-	F^-	PO_4^{3-}	SiO_2^{2-}
Inlet	<1-2	<1 -2	<1 - 2	<1	<1	2 - 20
Outlet	<1-2	<1 -2	<1 - 2	<1	<1	2 - 20

ICP-AES [ppb]

	Si_{tot}	K_{tot}	Na_{tot}	Cu_{tot}	Fe_{tot}	Cr_{tot}	Ni_{tot}	Co_{tot}	Zn_{tot}
Inlet	2 -3	<1	<1	<0.5	<0.5 -1	<1	<0.1	<0.8	0.3
Outlet	3 -6	<1	<1	<0.5	<0.5 -1	1 -4	0.5	<0.8	0.5

Typical impurity concentration range for tests with an inlet conductivity ≤ 0.06 µS/cm.

Tests with higher inlet conductivity (by addition of Na_2SO_4) only differ from this analysis in higher SO_4^{2} and Na^+ contents (according to the figure above).

Crack Length Measurement Methods

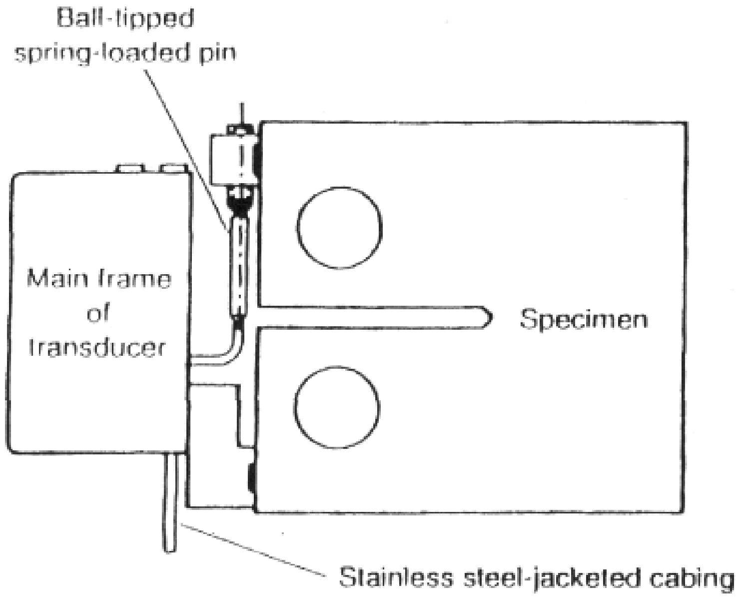

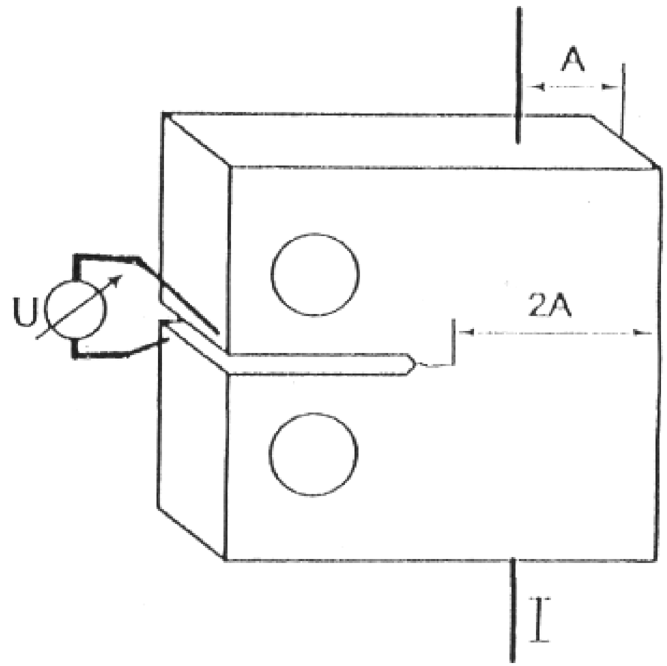

Compliance-Method

dCOD/dP = f (a)

Resolution: 50 –100 μm

DCPD-Method

$\Delta U = f(a)$

Resolution: 5 – 20 μm

Effect of Temperature

Time-dependent SCC Crack Growth under Static Load at 288 °C

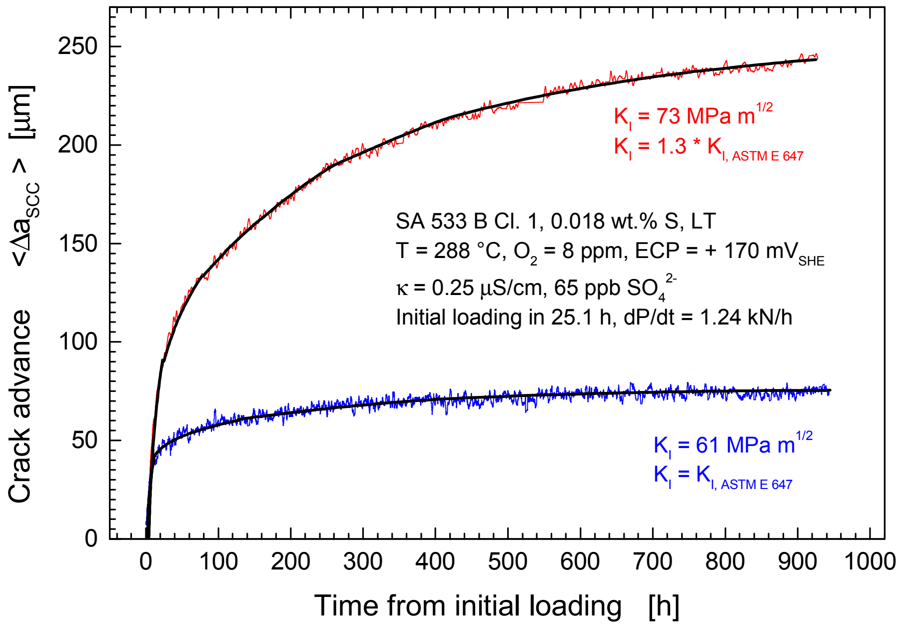

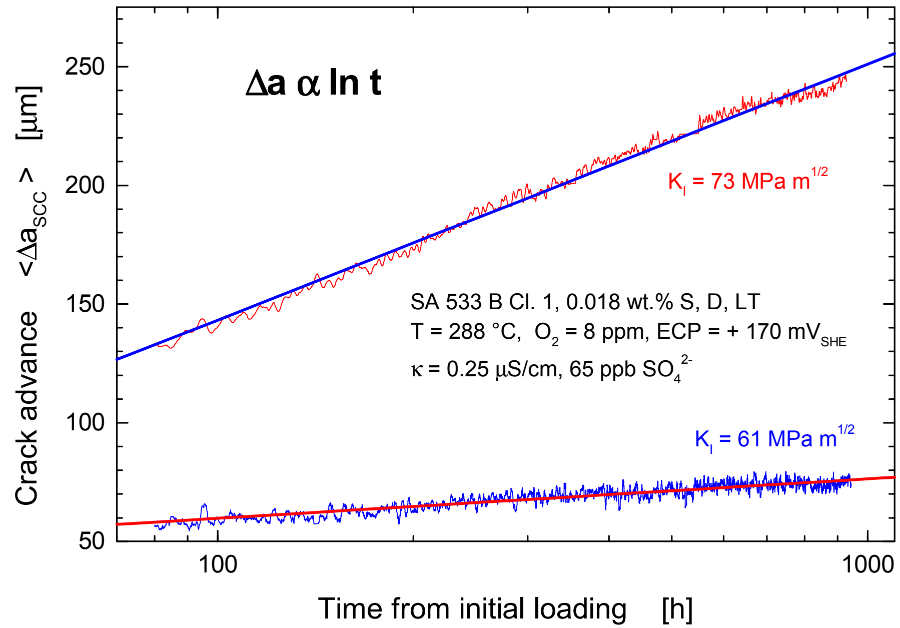

$\Delta a \propto \ln t \rightarrow$ indication that SCC crack growth under static loading is controlled by low temperature creep

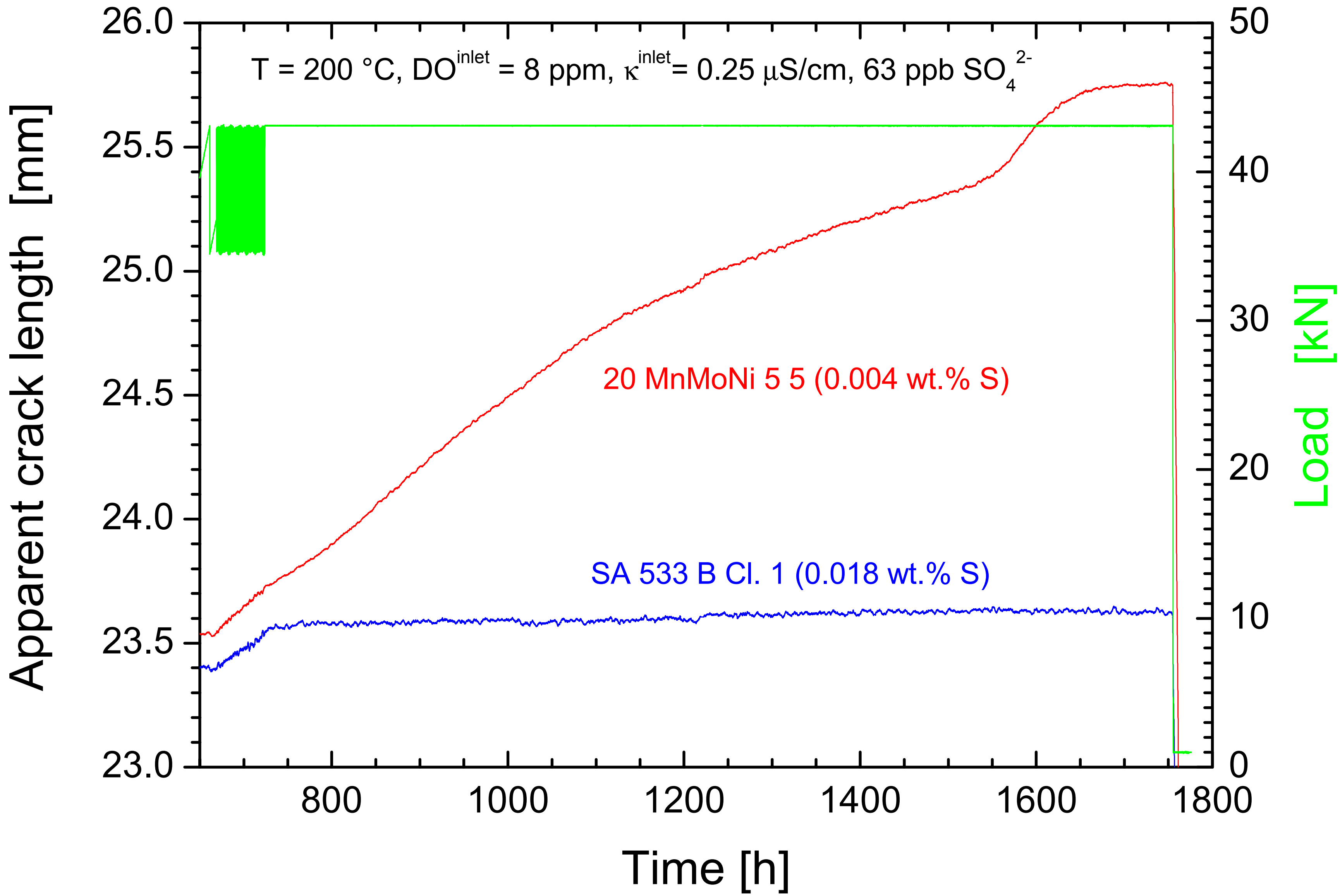
T = 200 °C, DO^inlet = 8 ppm, κ^inlet = 0.25 µS/cm, 63 ppb SO4^2-
20 MnMoNi 5 5 (0.004 wt.% S)
SA 533 B Cl. 1 (0.018 wt.% S)
Apparent crack length [mm]
Load [kN]
Time [h]
26.0
25.5
25.0
24.5
24.0
23.5
23.0
50
40
30
20
10
0
800
1000
1200
1400
1600
1800

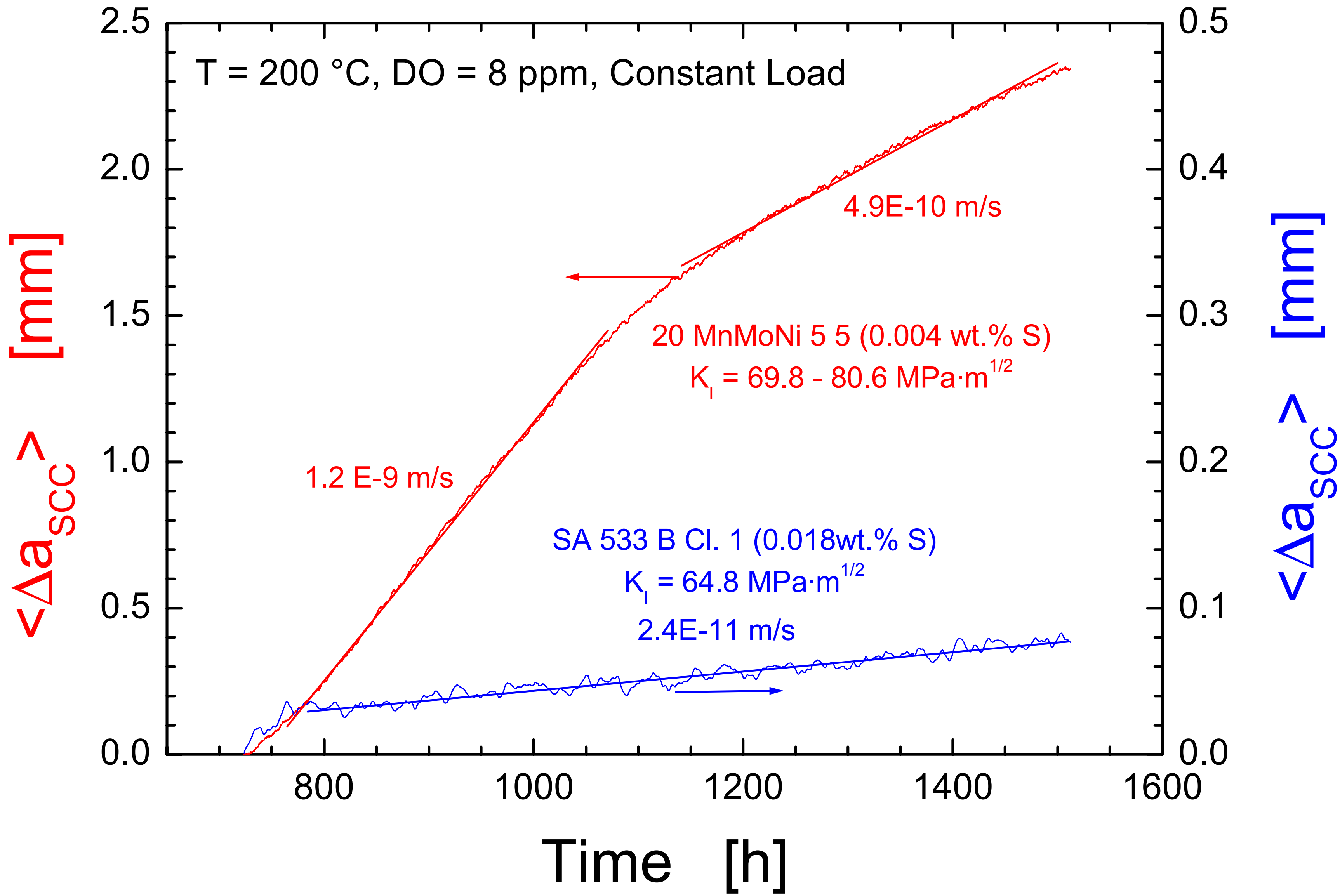
T = 200 °C, DO = 8 ppm, Constant Load
4.9E-10 m/s
20 MnMoNi 5 5 (0.004 wt.% S)
K$_I$ = 69.8 - 80.6 MPa·m$^{1/2}$
1.2 E-9 m/s
SA 533 B Cl. 1 (0.018wt.% S)
K$_I$ = 64.8 MPa·m$^{1/2}$
2.4E-11 m/s
<Δa$_{SCC}$> [mm]
Time [h]
2.5
2.0
1.5
1.0
0.5
0.0
0.5
0.4
0.3
0.2
0.1
0.0
800
1000
1200
1400
1600

SCC Crack Growth under Constant Load, High-Sulphur Steel

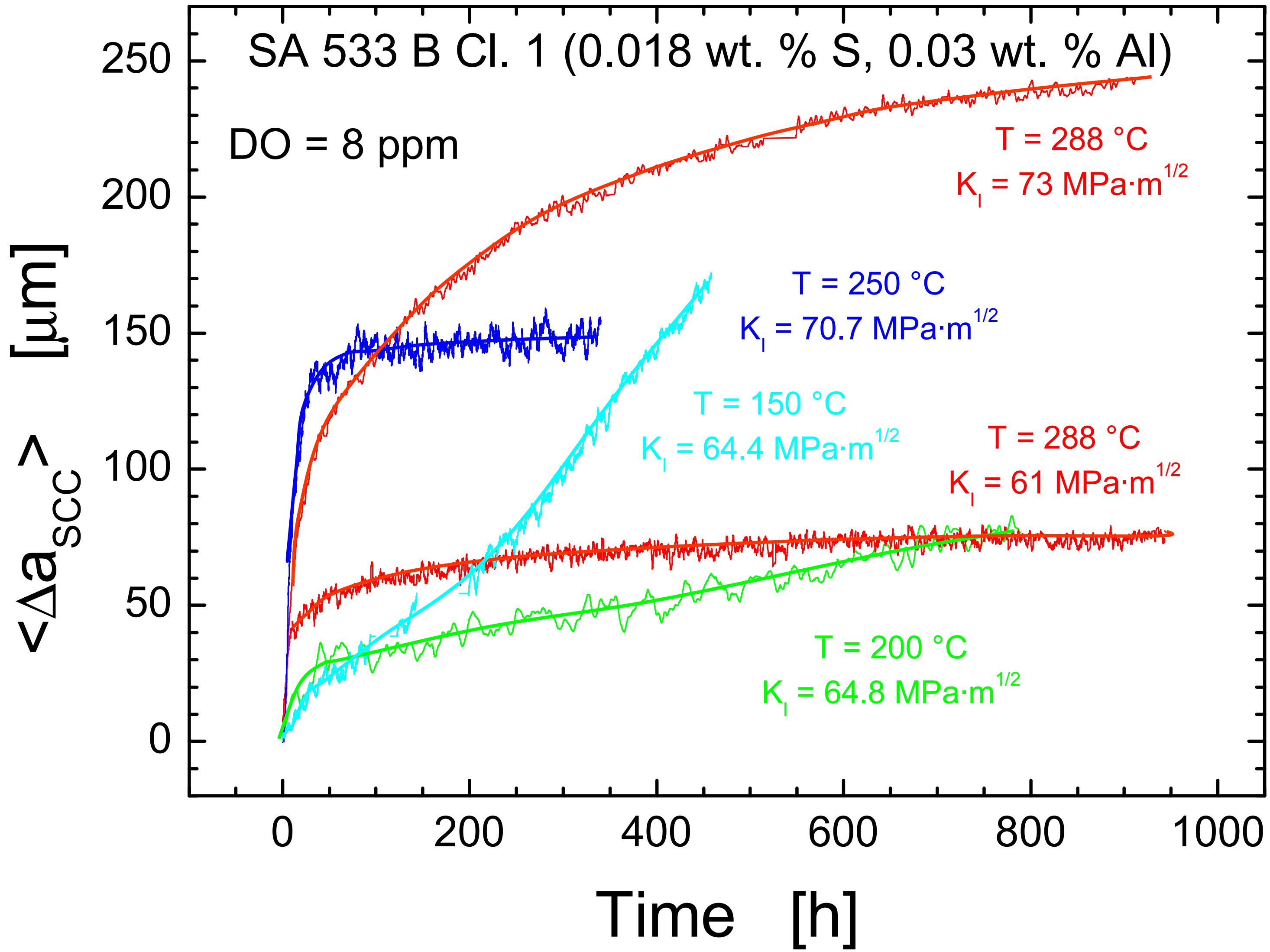

SCC Crack Growth under Constant Load, Low-Sulphur Steel

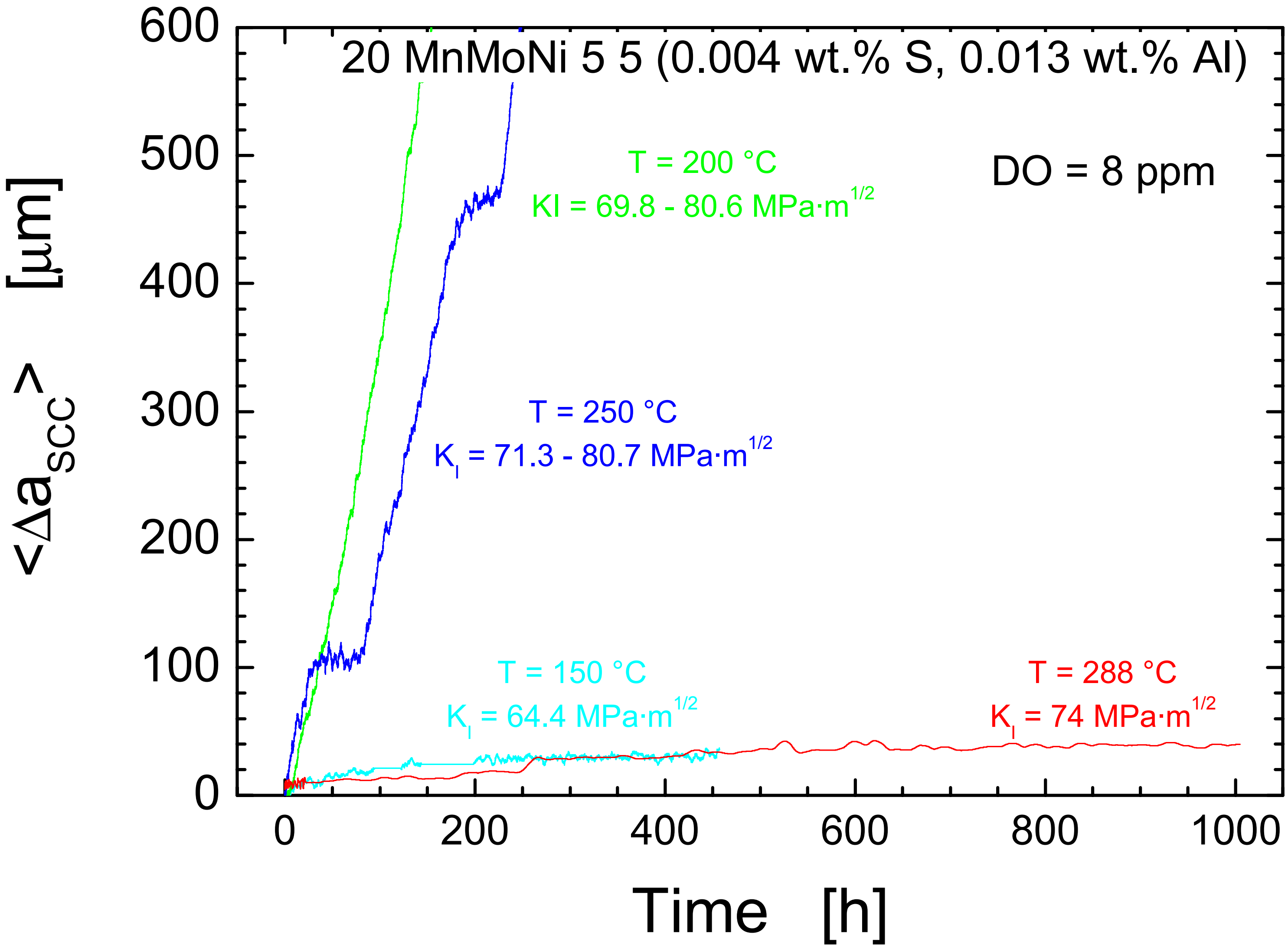

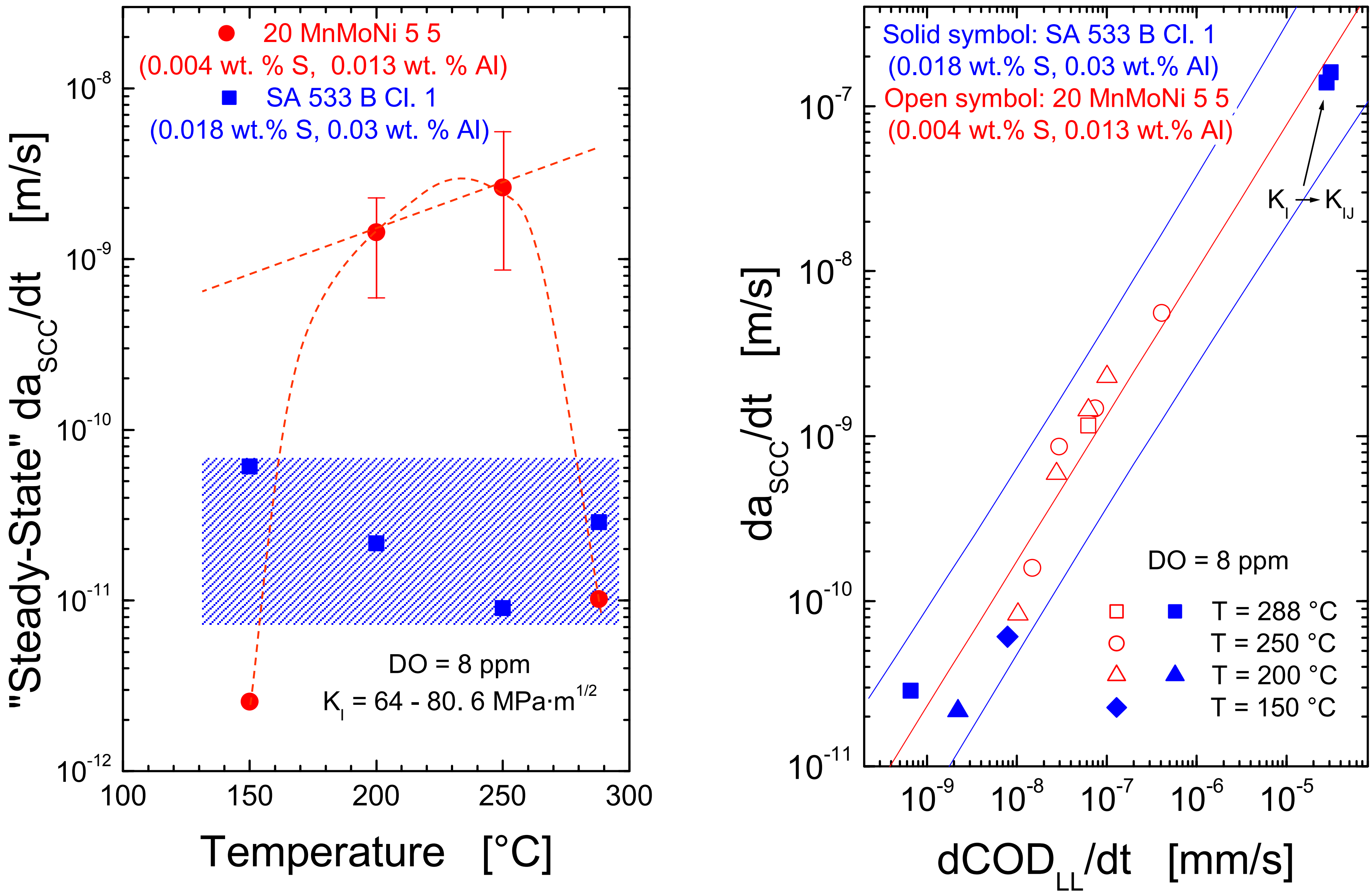

20 MnMoNi 5 5
(0.004 wt. % S, 0.013 wt. % Al)
SA 533 B Cl. 1
(0.018 wt.% S, 0.03 wt. % Al)
DO = 8 ppm
K_I = 64 - 80. 6 MPa·m^1/2
"Steady-State" da_SCC/dt [m/s]
Temperature [°C]
Solid symbol: SA 533 B Cl. 1
(0.018 wt.% S, 0.03 wt.% Al)
Open symbol: 20 MnMoNi 5 5
(0.004 wt.% S, 0.013 wt.% Al)
K_I → K_IJ
DO = 8 ppm
T = 288 °C
T = 250 °C
T = 200 °C
T = 150 °C
da_SCC/dt [m/s]
dCOD_LL/dt [mm/s]

Comparison with Disposition Lines and Literature Data

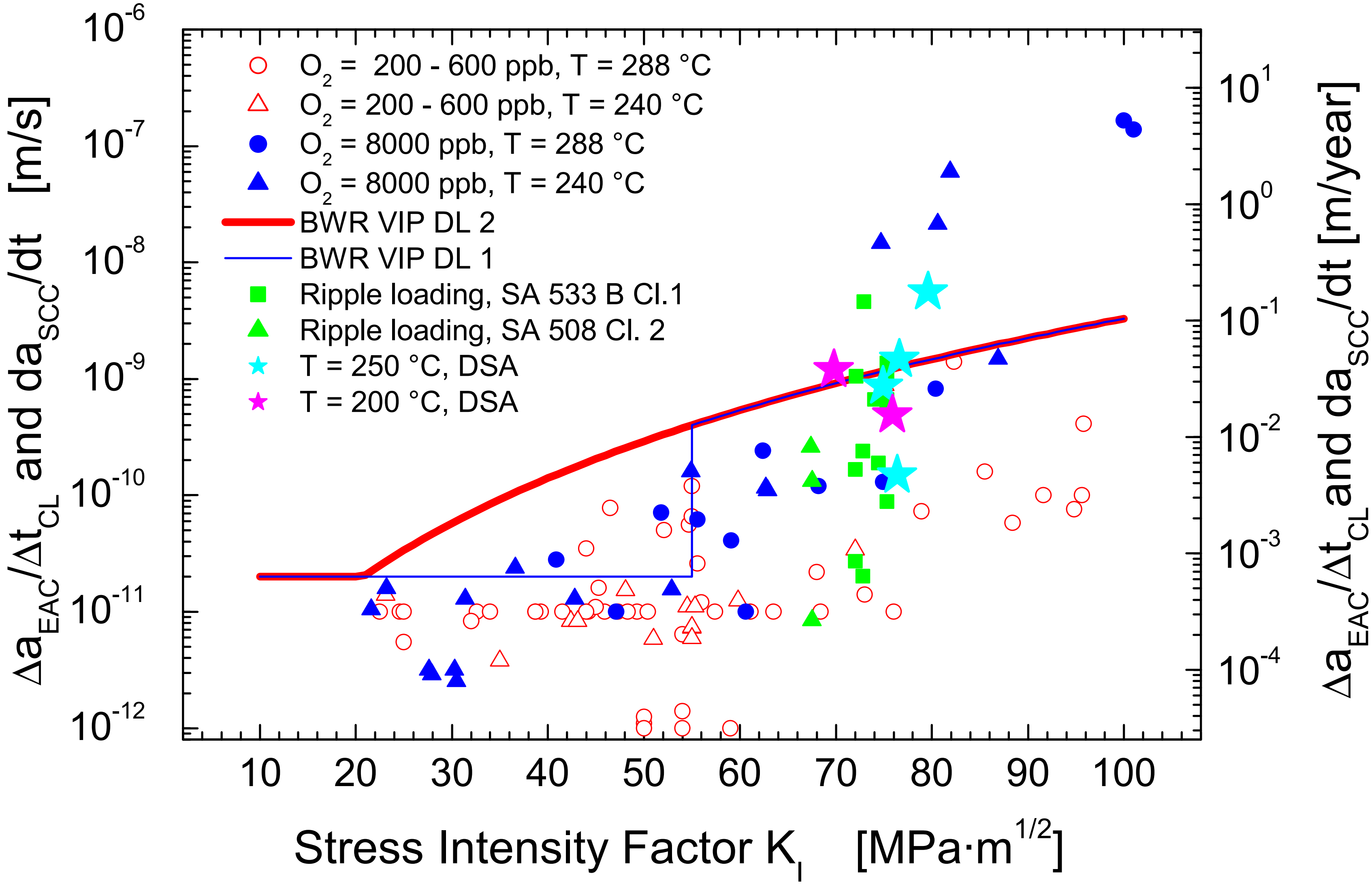

Dynamic Strain Ageing

20 MnMoNi 5 5 (0.004 wt.% S, 0.013 wt.% Al)

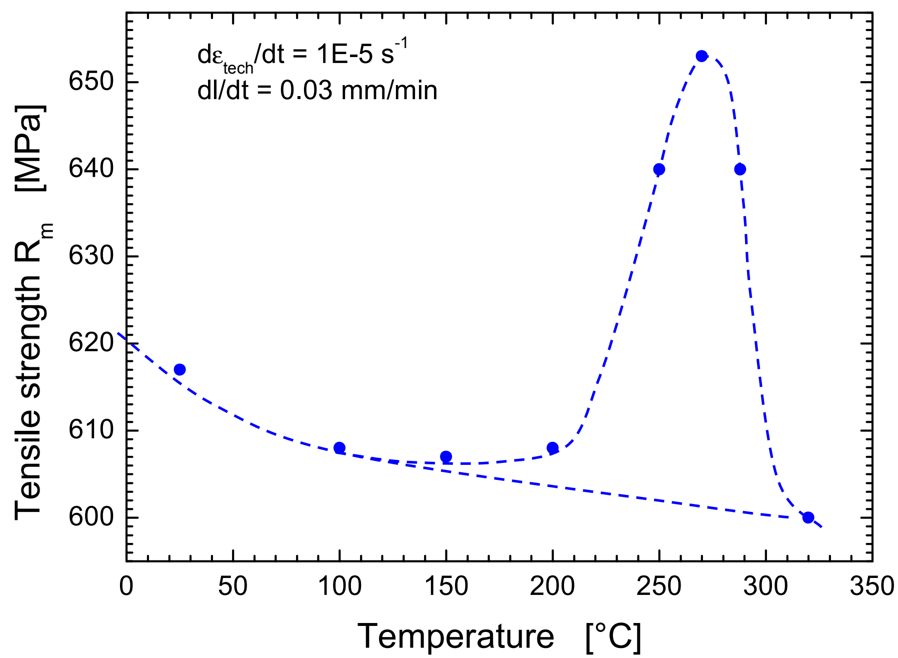

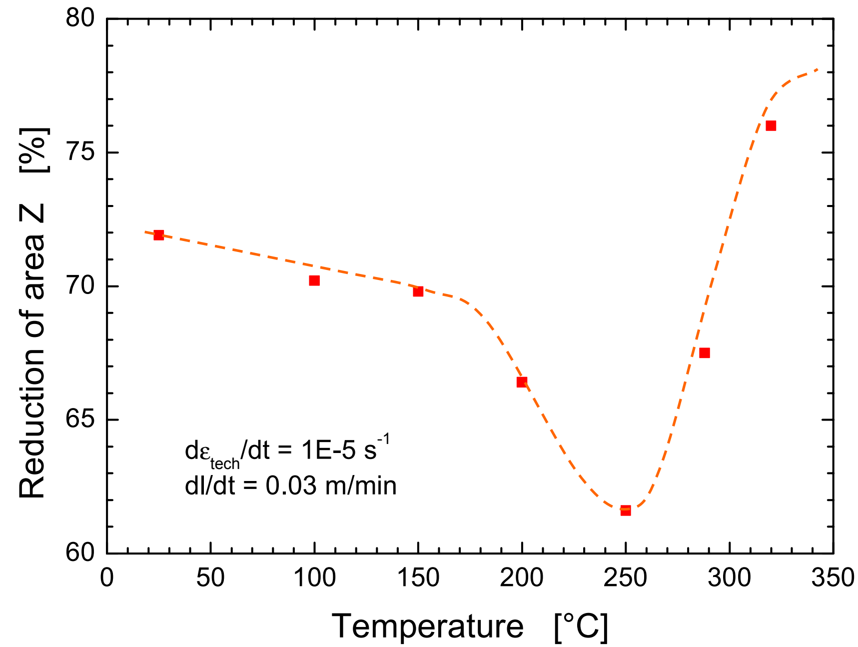

Dynamic Strain Ageing

20 MnMoNi 5 5 (0.004 wt.% S, 0.013 wt.% Al)

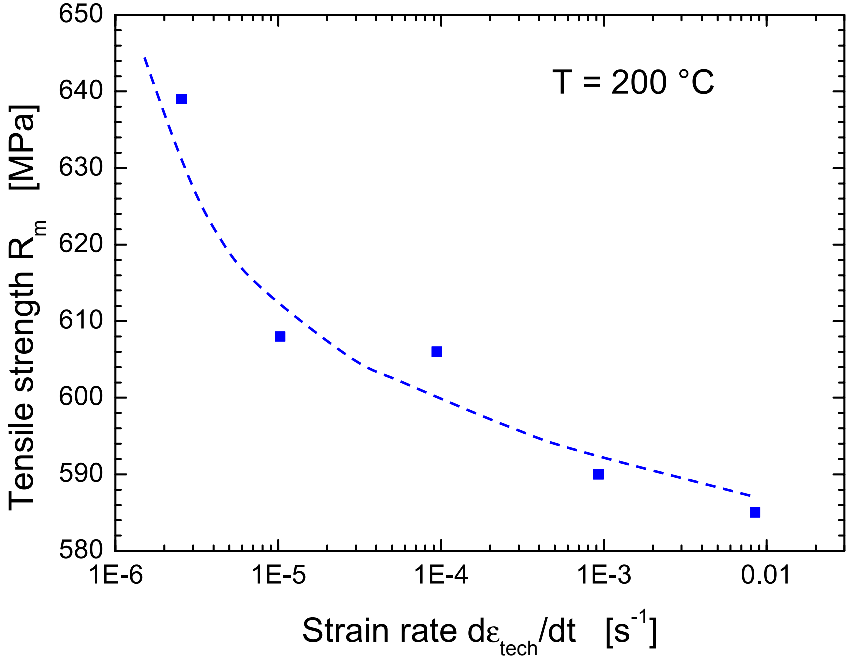

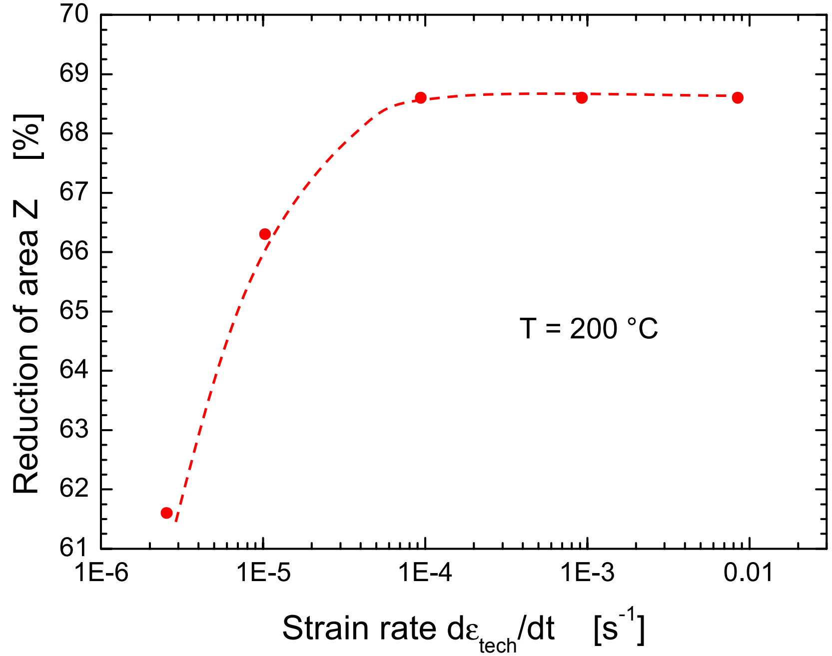

Dynamic Strain Ageing: Serrated Flow

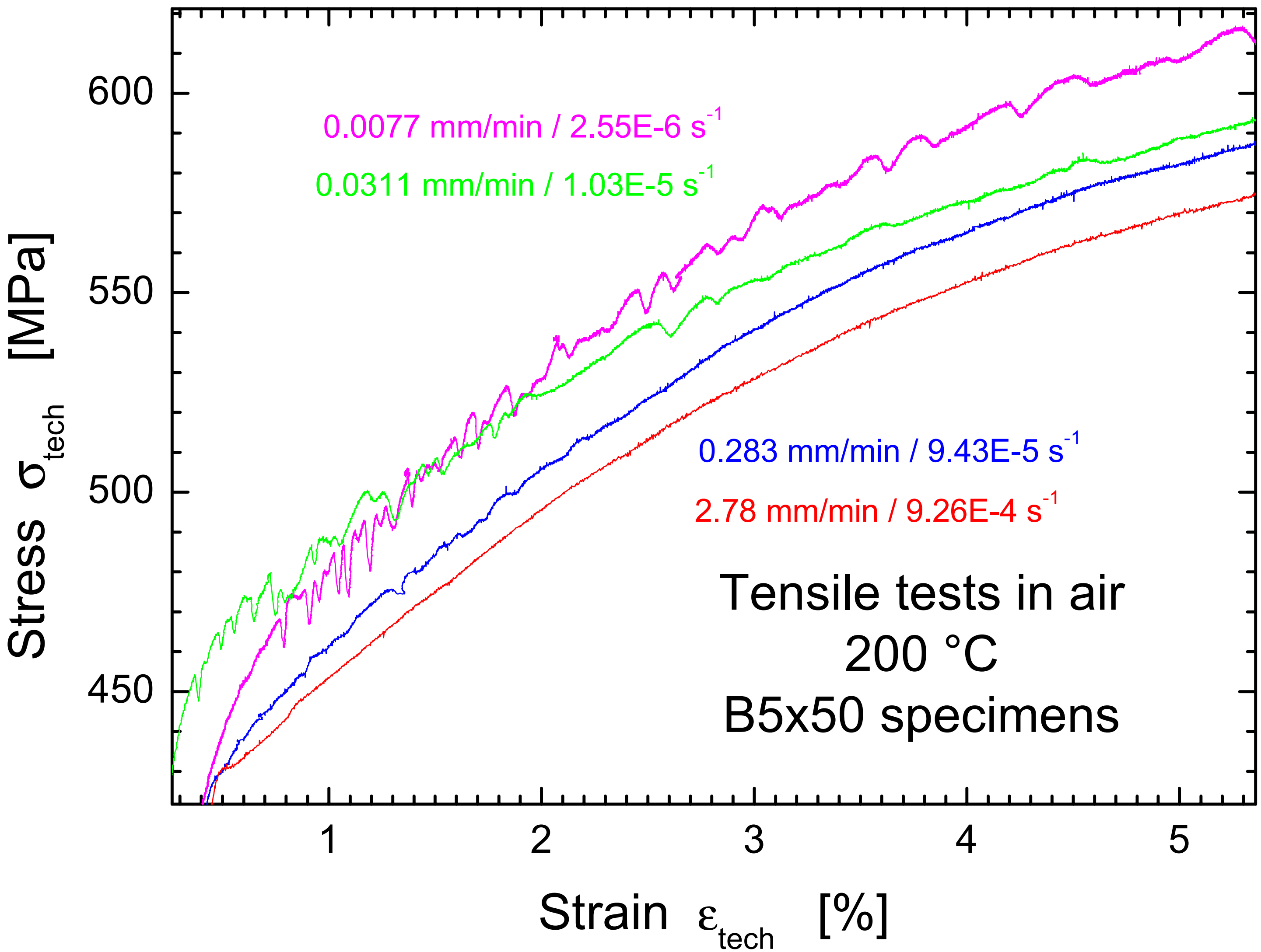

Effect of Water Chemistry and Oxygen Transients

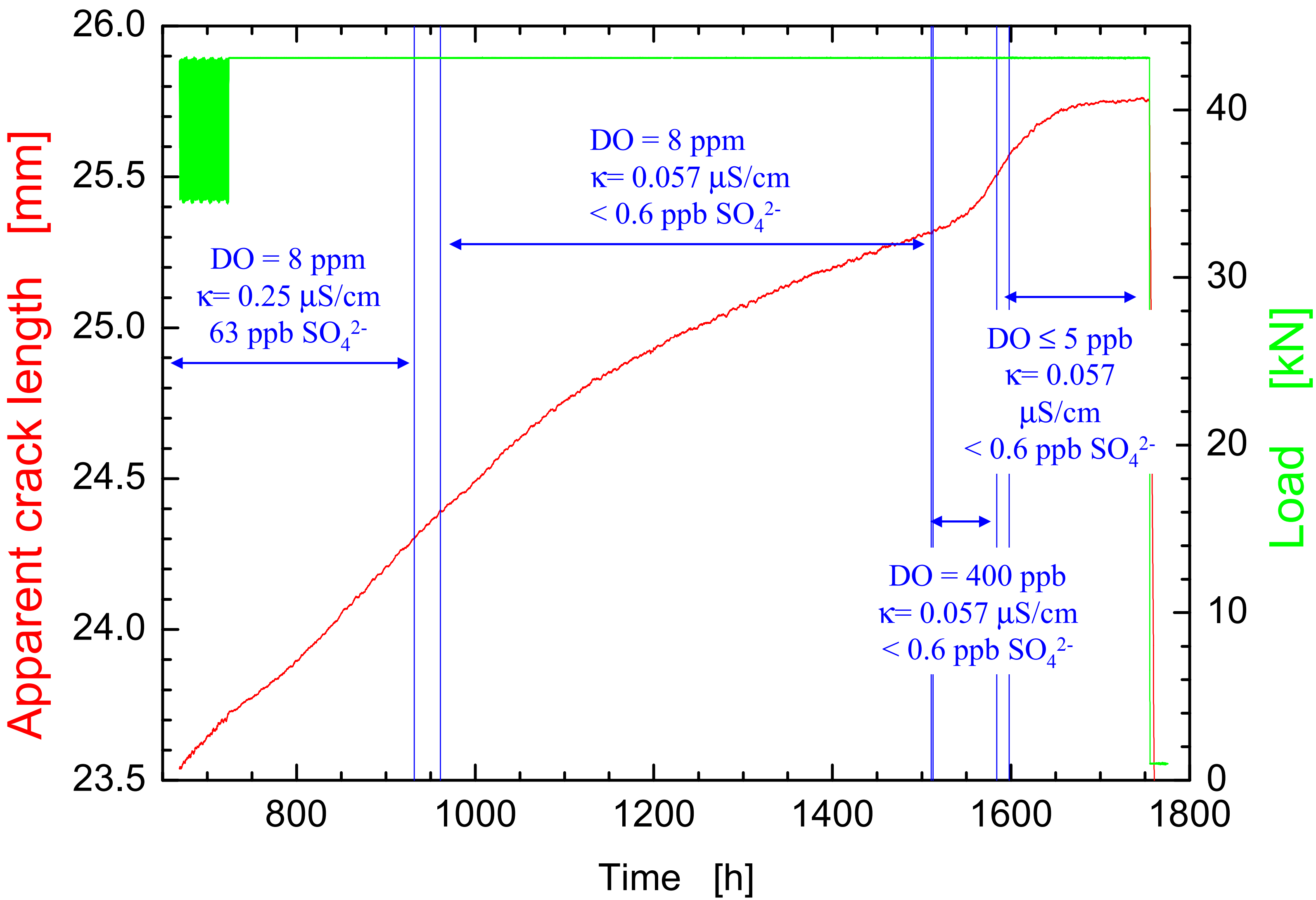

Effect of Water Chemistry and Oxygen Transients

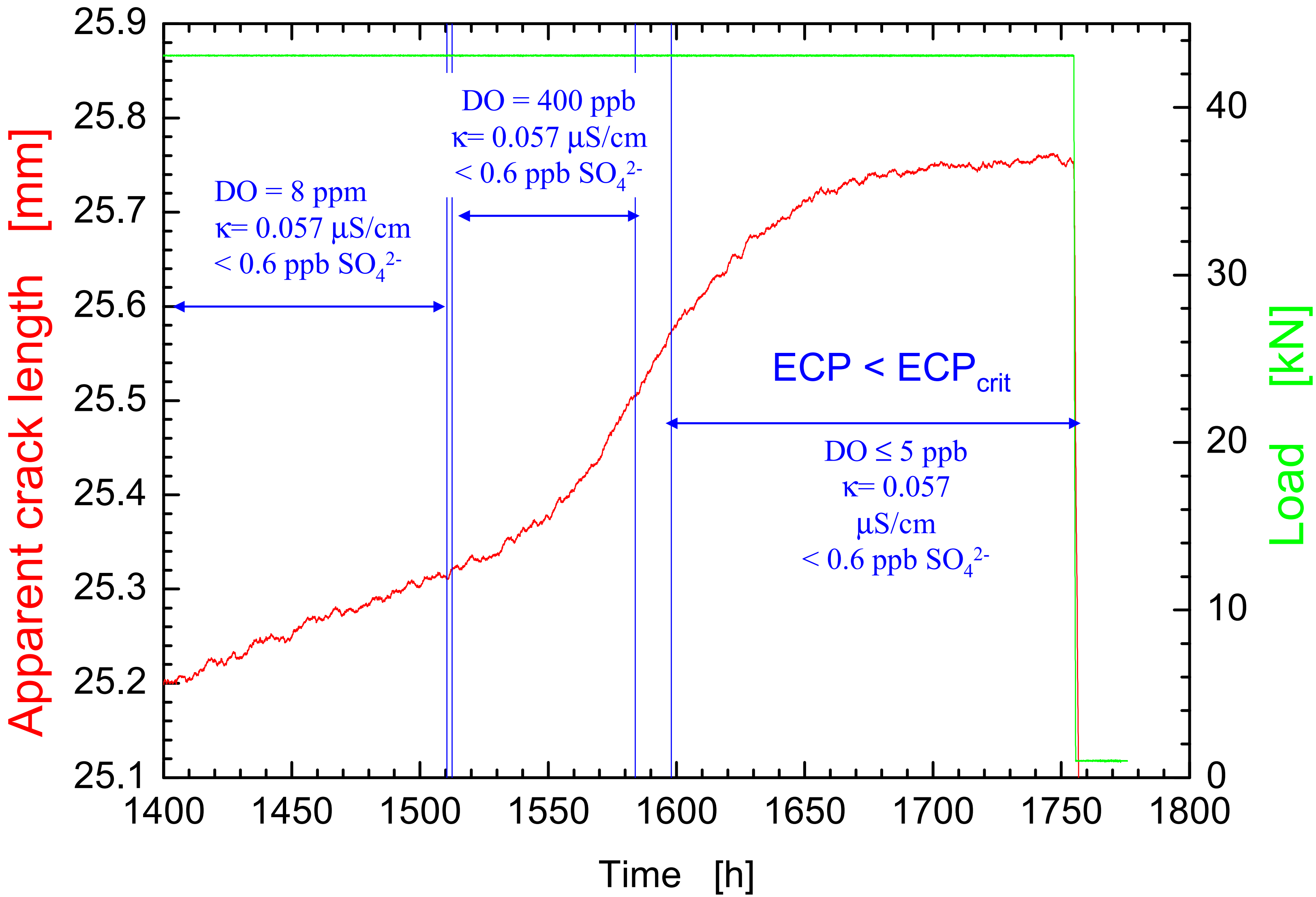

Ripple Loading

Ripple Loading

- → Small temperature and pressure fluctuations during stationary power operation

- T = 288 °C, DO^{inlet} = 8 ppm, κ^{inlet} = 0.066 µS/cm, SO_4^{2-} < 0.6 ppb

  SA 533 B Cl. 1 (0.018 wt.% S, TS) : ECP = + 215 mV_{SHE}

  SA 508 Cl. 2 (0.004 wt.% S, TL) : ECP = + 184 mV_{SHE}

- Constant load amplitude, load control, positive saw tooth

  Δt_{Rise} = 0.01 h – 10 h, Δt_{Fall} = 0.01 h

  ν = 1.4 E-2 Hz – 2.7E-5 Hz

  R = 0.957 - 0.970

  ΔK = 2.0 $MPa \cdot m^{1/2}$ - 3.3 $MPa \cdot m^{1/2}$

  K_I^{max} = 66.7 $MPa \cdot m^{1/2}$ - 75.3 $MPa \cdot m^{1/2}$

  $K_I^{max}/K_{I,\ ASTM\ E647}$ = 0.9 - 1.07

  $K_I^{max}/K_{I,\ ASTM\ E399}$ = 1.26 - 1.5

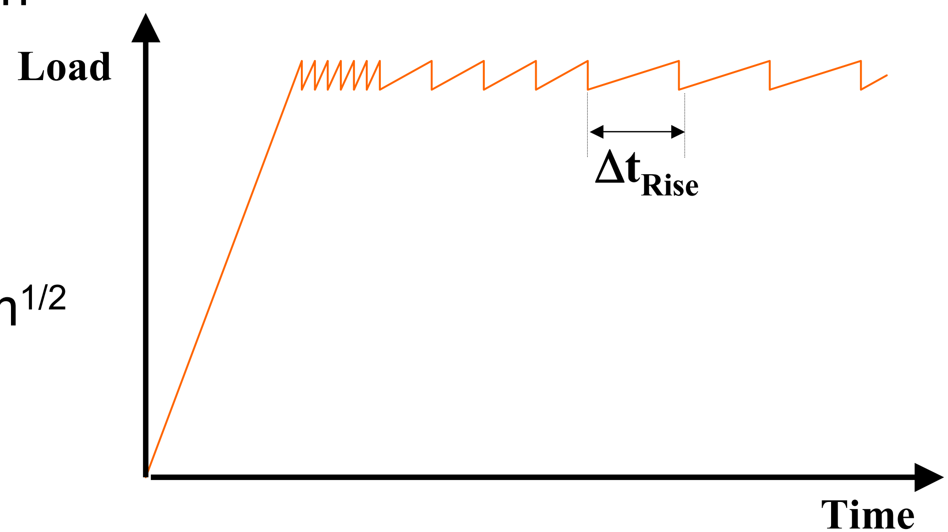

Ripple Load

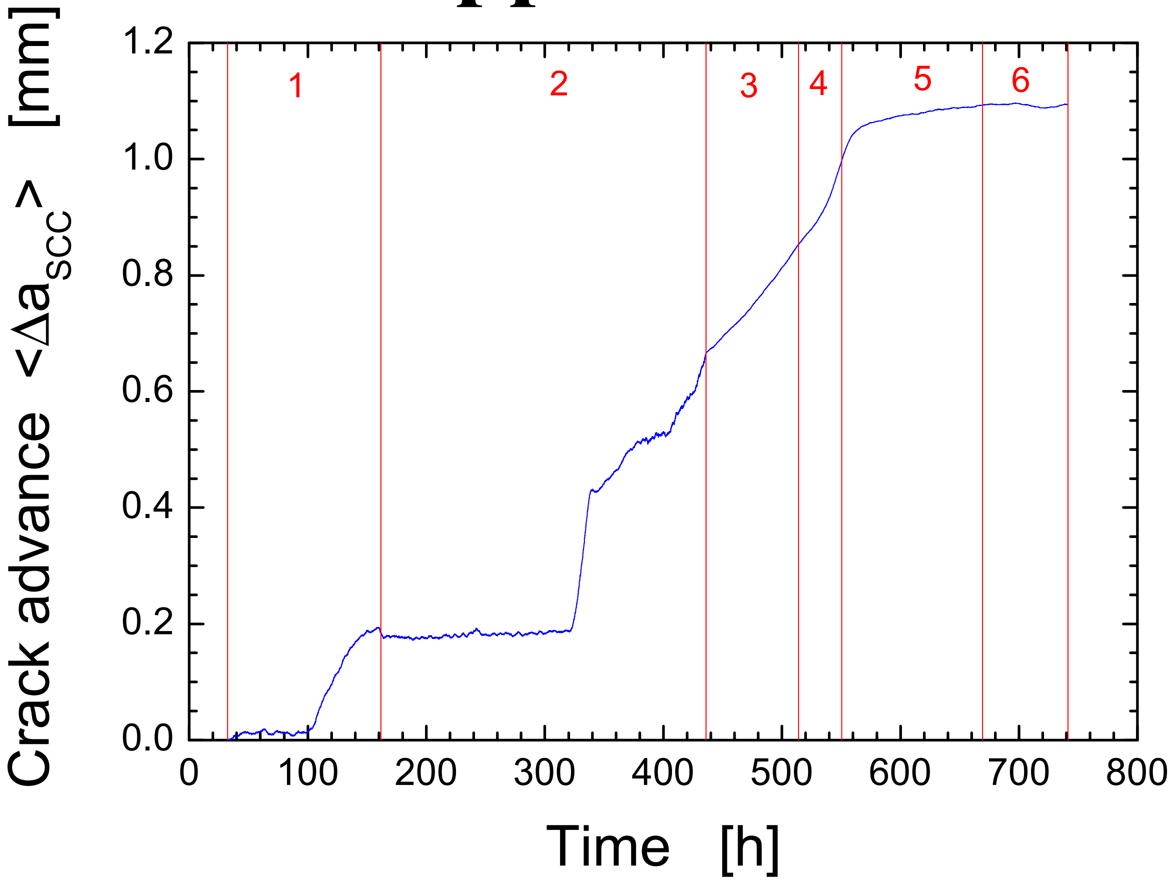

Phase	1	2	3	4	5	6
Δt_R [h]	0.01	0.1	1	0.7	7	10
ν [Hz]	1.4E-2	2.5E-3	2.7E-4	3.8E-4	3.9E-5	2.74E-5
R [-]	0.957	0.957	0.957	0.970	0.970	0.957
ΔK [MPa·m$^{1/2}$]	3.1	3.2	3.3	2.3	2.3	3.3

Ripple Load

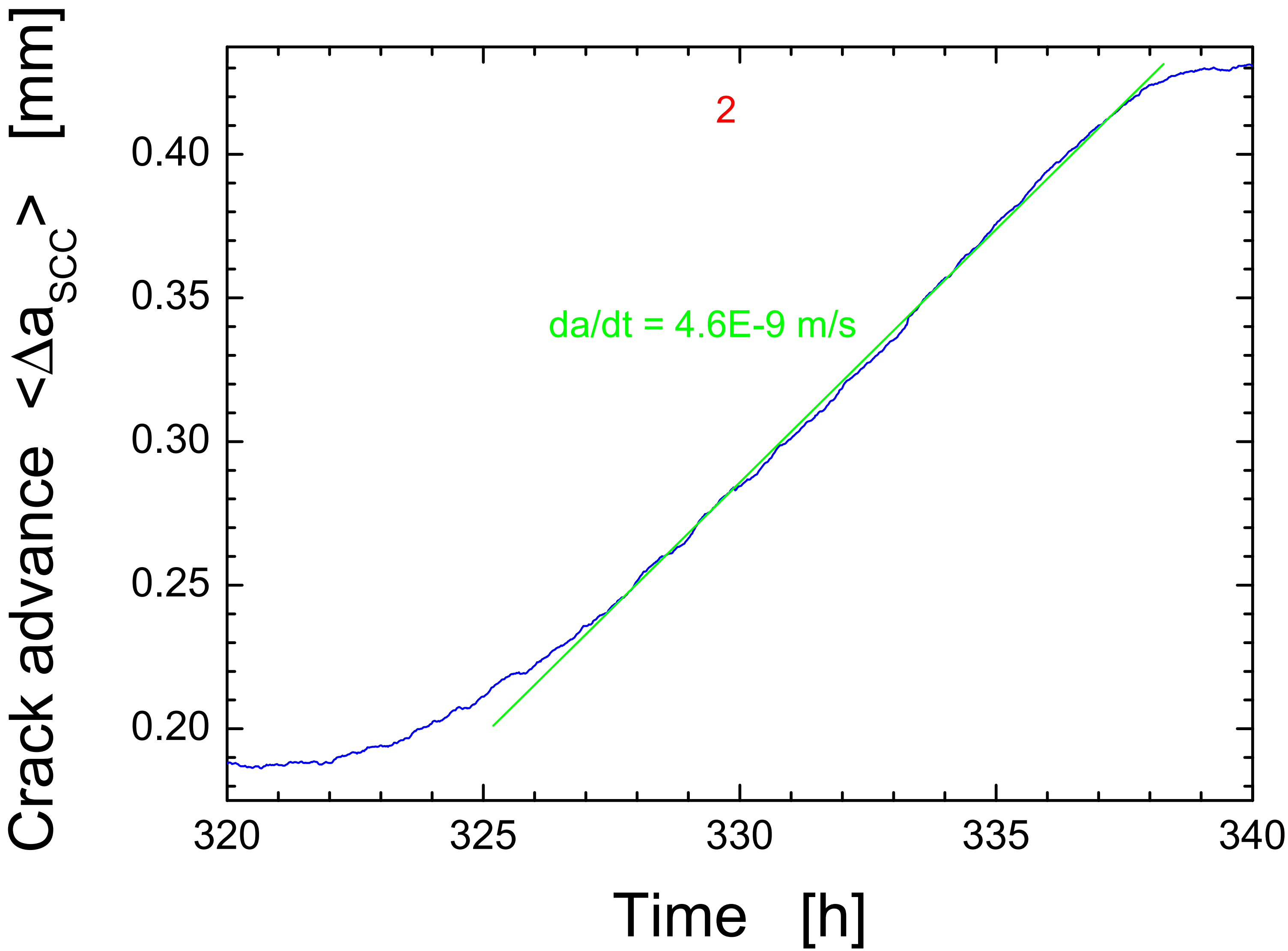
Crack advance $<\Delta a_{SCC}>$ [mm]
0.20
0.25
0.30
0.35
0.40
2
da/dt = 4.6E-9 m/s
320
325
330
335
340
Time [h]

Ripple Load

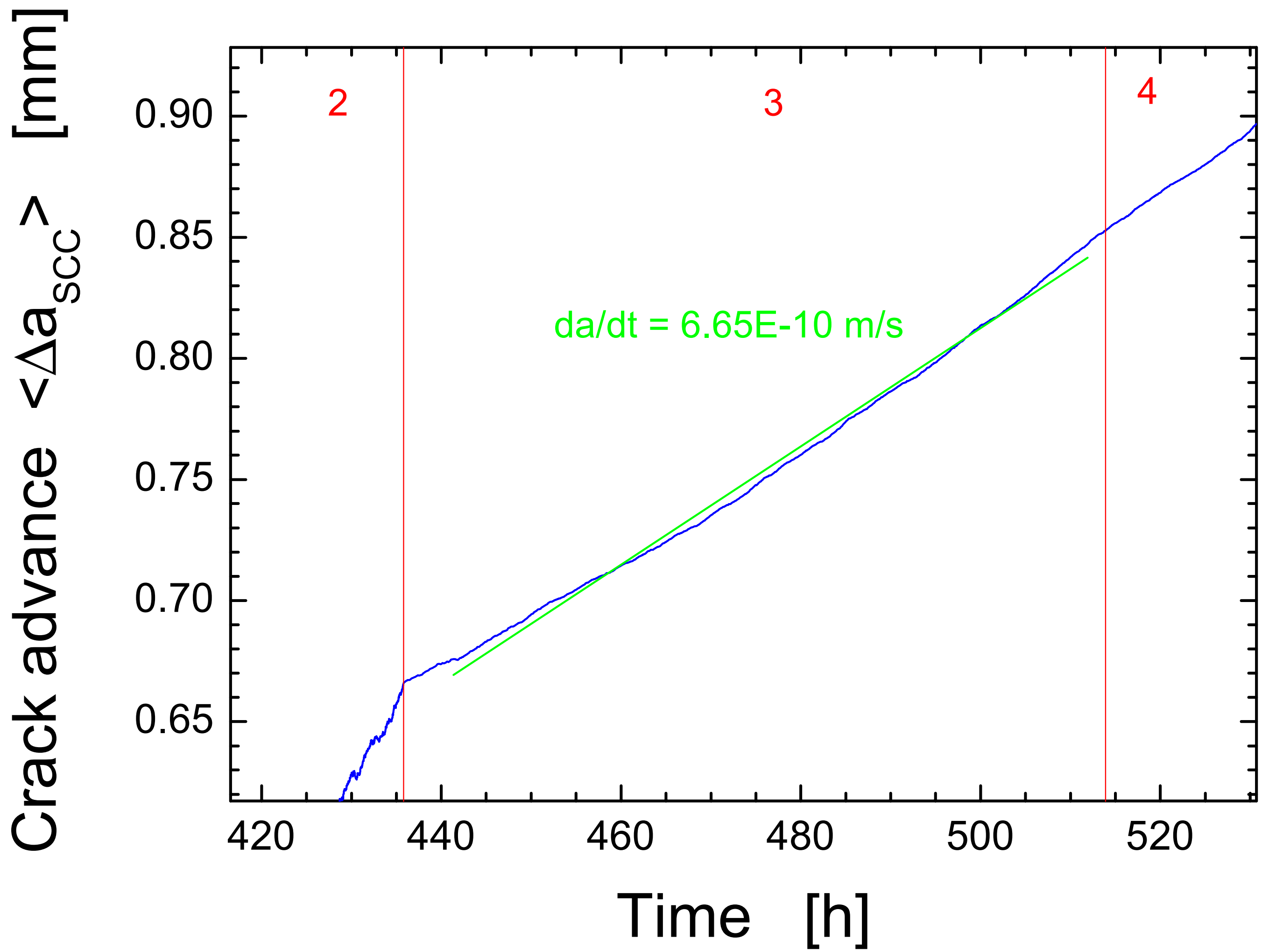

Crack advance <Δa$_{SCC}$> [mm]
0.90
0.85
0.80
0.75
0.70
0.65
2
3
4
da/dt = 6.65E-10 m/s
420
440
460
480
500
520
Time [h]

Ripple Load vs. Constant Load

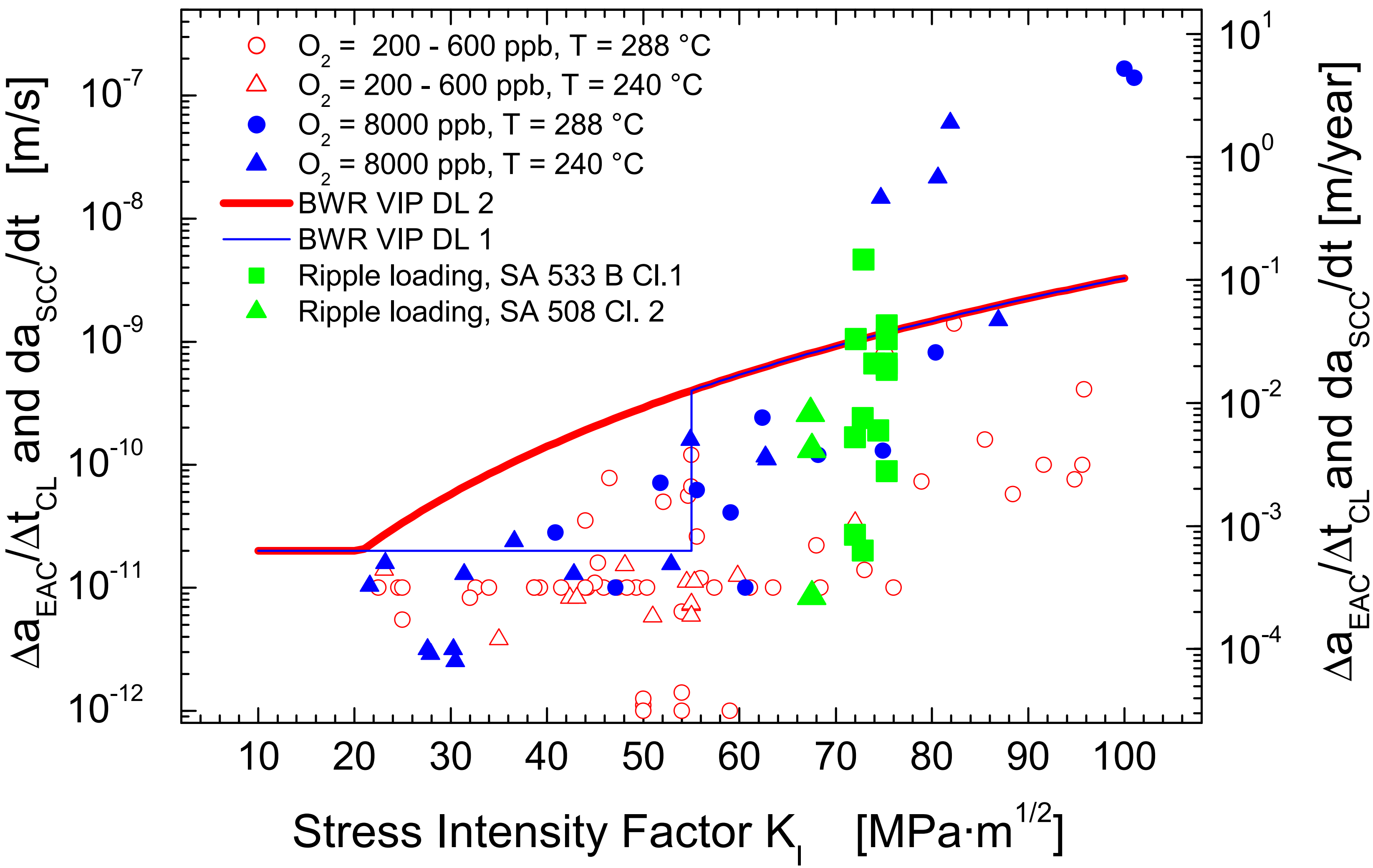

Comparison with ASME XI

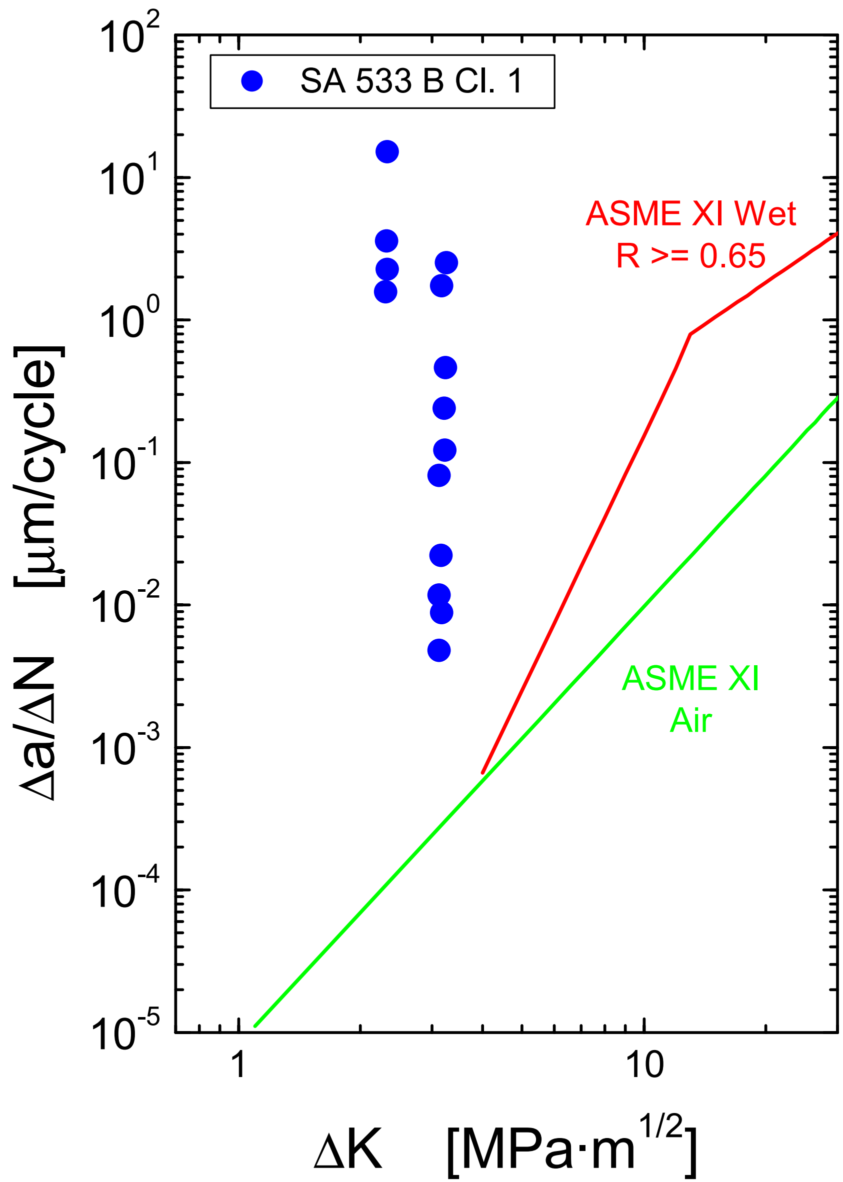

Ripple Load vs. SRL + LCF Tests

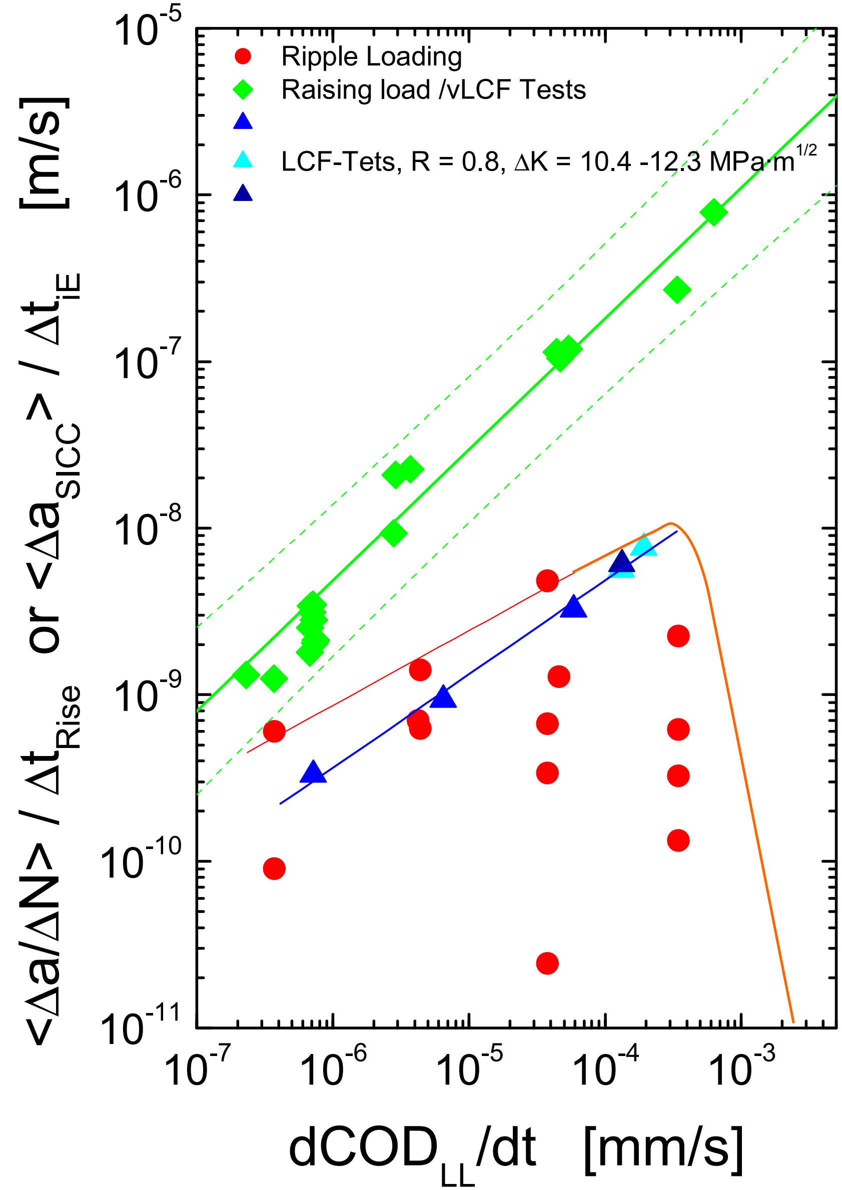

Effect of Microstructure

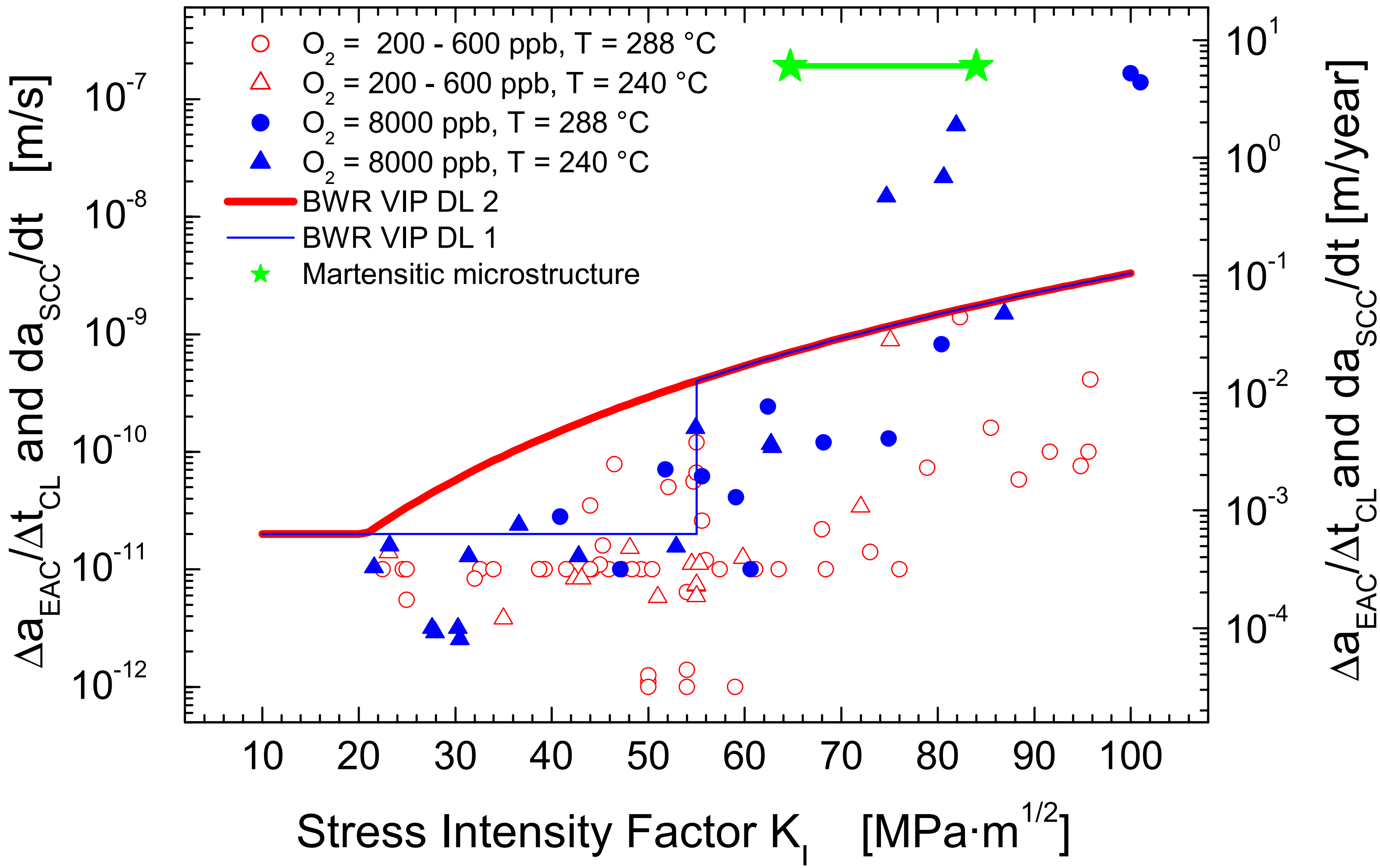

Summary (SCC I + II, RIKORR) of SCC Crack Growth

- **T ≈ 288 °C**

Sustained (steady-state) SCC crack growth for:

- Ripple Loading / Periodical Partial Unloading
- SO_4^{2-} + Cl^- ≥ ≈ 500 ppb (e.g. > EPRI action level 3)
- $K_I \rightarrow K_{IJ}$ wt.% S↑, R_p↑, DSA↑(N/Al↑) → K_{IJ} ↓
- $P \rightarrow P_{\text{plastic limit load}}$ or $\sigma_{\text{net section}} \rightarrow R_p$
- Excessive hardness (>≈ 350 HV), martensitic microstructure,

Otherwise: Decay of SCC crack growth and crack arrest or very slow crack growth rates (≤ some few hundred µm/year)

- **T = 200 – 250 °C**

20 MnMoNi 5 5 (0.004 wt.% S, 0.013 wt.% Al):
SCC-CGR ≈ "Low Sulphur Line" ≡ BWR VIP Disposition Line 2
Possible DSA-effect?

Conclusions I

1. The conservative character of the BWR VIP SCC Disposition Lines for LAS has been further confirmed for
   - RPV base material, Q + T + SR
   - SSY + static load
   - T ≈ 288 °C + water chemistry within current EPRI guidelines

2. The BWR VIP SCC DL may be exceeded
   - at lower (intermediate) temperatures + a susceptible material (DSA?)
   - small load fluctuations (ripple loading)

3. Preliminary indications for a possible effect of DSA on EAC

Conclusions II

→ BWR VIP SCC DL still seem to be adequate and conservative for the RPV (unaffected base material) for transient-free, steady-state power operation

→ Concern for
- feedwater nozzle
- weld and weld HAZ material
- material in the as-welded condition without PWHT
- materials with a low Al-content

Further testing

- at intermediate temperatures
- with weld and weld HAZ material
- with ripple loading or periodical partial unloading

for verification of BWR VIP SCC DL

Outlook

1. Effect of temperature and microstructure:

- RPV weld material
  - Circumferential girth weld of Biblis C (PWR, 1200 MWe, 1976)
  - 0.0058 wt. % Al $\rightarrow$ DSA?
- Weld heat-affected zone and simulated HAZ
  - 1T C(T)
  - 1T Blunt Notch C(T)
- Base material
  - Intermediate T + $K_I\downarrow$

2. Ripple loading / periodical partial unloading

- $\Delta K\downarrow$, $K_I^{max}\downarrow$

Acknowledgment

The presented work has been financially supported by the

Swiss Federal Nuclear Safety Inspectorate (HSK)

and

Swiss Federal Office of Energy (BFE)